GRANT AGREEMENT NUMBER: 323378
PROPOSAL ACRONYM: *GOTA*
PROJECT FULL TITLE: ***G****REATER* ***O****PERATING* ***T****EMPERATURE* ***A****LLOY*
FUNDING SCHEME: FP7-JTI-CS
DATE OF LATEST VERSION OF ANNEX I: *05/02/2013*
PERIOD NUMBER: 3 (START DATE: 1/3/15 END DATE: 30/4/2016)
PROJECT COORDINATOR: *ROGER THOMAS, TIMET UK LTD (email: roger.thomas@timet.com)*

MILESTONE 7: RESULTS OF TESTING AND CHARACTERISATION

LIST OF PARTICIPANTS:

PARTICIPANT NO.	PARTICIPANT ORGANISATION NAME	COUNTRY
1 (COORDINATOR)	TIMET UK LTD.	UNITED KINGDOM
2	FORGITAL ITALY S.P.A.	ITALY
3	DERITEND INTERNATIONAL LTD.	UNITED KINGDOM
4	SWANSEA UNIVERSITY	UNITED KINGDOM

1. Introduction:

1 (a) Milestone 7.

The GOTA project has completed its third period of performance with the testing of sample materials manufactured to represent cast, forged and welded components. Milestone 7 is a report summarizing all the testing and characterization performed in the project.

1 (b) Project Context and Objectives.

The GOTA project selected Timetal 834 (Ti-834) as the candidate titanium alloy for long term service use in aero engine intermediate compressor casing (ICCs) at temperatures 50°C higher than those currently applied to alloy Ti-6242S, and then manufacture and test the Ti+ alloy. The partners have demonstrated the industrial scale manufacture of this titanium alloy as castings and as rolled rings; sheet and weld wire, and demonstrated the fabrication by laser welding of the alloy,

Swansea University has undertaken a programme of testing and characterization of these materials, both characterizing the materials as manufactured, and evaluating the durability of the materials after exposure to the proposed operating temperature for extended periods.

1 c) Metallurgical Background

In ICC applications Ti-834 alloy would be required to operate at temperatures approaching 500°C, which is approximately 50°C higher than is currently possible using the Ti-6242S alloy. The replacement alloy will also need to demonstrate suitable mechanical properties after prolonged exposure at operating temperatures.

Near alpha (α) titanium alloys such as Ti-6242S are used extensively for intermediate temperature applications such as gas turbine ICCs. These types of high temperature alloys are selected due to their balance of strength, fatigue and creep properties. However after prolonged exposure to high temperatures these titanium alloys are known to experience a reduction in mechanical properties [1], [2],[3], [4],[5]. The reduction in fatigue and creep performance is essentially attributed to the formation of α case at the surface of the alloy. Reductions in ductility are not so well understood and cannot solely be correlated with the formation of α-case. Previous studies [1],[6] have attributed the loss in ductility to the precipitation of coherent Ti_3Al or α_2 particles in conjunction with the formation of silicides.

Ti-834 was initially developed as a wrought alloy [7] with an α plus transformed beta (β) structure for blade and disk applications[8]. It was initially designed to maximize creep and low cycle fatigue performance up to temperatures of approximately 600^{o}C through a combination of alloying and heat treatment. In contrast to the wrought material the cast form of Ti-834 exhibits a fully transformed β

microstructure. The variation in microstructure results in a different balance of mechanical properties to the forged material. Strength levels at room and elevated temperatures comparable to wrought material are possible, while the cast alloy also provides better creep resistance than its wrought equivalent[8], although with lower room temperature ductility. The low cycle fatigue performance of the cast alloy is inferior to that of the wrought form of the alloy[9].

2. Experimental Procedures

2.1 Material

The materials under investigation during this project were Ti-6242S and Ti-834. Centrifugal cast Ti-6242S and Ti-834 was produced and supplied by Doncaster Settas. Gravity cast Ti-834 was produced and supplied by Birmingham University. Forged Ti-834 was produced and supplied by Forgital, Italy S. P. A. Sheet forms of Ti624S and Ti-834 were supplied by TIMET. The laser welding operation was performed by Trollhattan University, Sweden on material supplied by TIMET.

2.2 Testing Plan

The initial testing plan for the project is illustrated in figure 1. The testing plan included tensile, creep, low cycle fatigue, fatigue crack propagation and fracture toughness tests. These tests were to be performed at room and elevated temperatures (Ti-6242S 450^{o}C, Ti-834 500^{o}C) on unexposed specimens and specimens which were exposed in air for 1000 hours at their testing temperature.

MATERIAL TYPE	Macro	Micro	EBSD	RTT, after 1000hrs HT @450oC,	RTT	**RTT post 1000hrs @500oC.**	ETT @ 500oC	ETT @ 450oC	ETT @450C after 1000hrs HT at 450C	**ETT 500oC post 1000hrs @500oC.**	Creep two different loads, 500oC	Creep two different loads, 450oC	Creep, two different loads, 500C, after 1000hrs HT @500C	LCF RT	LCF 450oC	LCF 500oC	LCF RT, after 1000hrs HT @500C	LCF 500C, after 1000hrs HT @500C	FCP RT (R=0.1)	FCP 500oC (R=0.1)	Fracture Toughness	FCP 450oC (R=0.1)
Ti+ Rings: Ring 5: SHTA	2	4	1	0	2	**2**	2	0	0	**2**	4	0	4	6	0	6	6	6	1	1	2	
Ti+ Rings: Ring 4: SHTA	1	2	1	0	2	**1**	1	0	0	**1**	0	0	0	0	0	0	0	0	0	0	0	
Ti+ Rings: Ring 3: SHTA	1	2	1	0	2	**1**	1	0	0	**1**	0	0	0	0	0	0	0	0	0	0	0	
Ti 6242S CentCast+HIP+SHTA: 1.8 - 2.0mm	1	2	0	2	2	**0**	0	2	2	**0**	0	4	0	0	0	0	0	0	1	1	0	1
Ti 6242S CentriCast+HIP+SHTA: 8 - 10mm	1	1	**0**	**1**	**1**	**0**	**0**	**1**	**1**	**0**	**0**	**0**	0	**6**	**6**	**0**	0	0	**1**	**1**	0	**1**
Ti 6242S Centricast+HIP+SHTA: 20 - 22mm	1	1	**0**	**1**	**1**	**0**	**0**	**1**	**1**	**0**	**0**	**0**	0	**0**	**0**	**0**	0	0	**1**	**1**	0	**1**
Ti 6242S CentCast+HIP+SHTA: 25 - 35mm	1	2	0	2	2	**0**	0	2	2	**0**	0	4	0	6	6	0	0	0	1	1	2	1
Ti + Heat One, As CentCast + SHTA: 8 - 10mm	0	0	0	0	0	**0**	0	0	0	**0**	0	0	0	0	0	0	0	0	0	0	0	
Ti + Heat One, As CentCast + SHTA: 25 - 35mm	0	0	0	0	0	**0**	0	0	0	**0**	0	0	0	0	0	0	0	0	0	0	0	
Ti + Heat Three, As GravCast + SHTA: 8 - 10mm	0	0	0	0	0	**0**	0	0	0	**0**	0	0	0	0	0	0	0	0	0	0	0	
Ti + Heat Three, As GravCast + SHTA: 25 - 35mm	0	0	0	0	0	**0**	0	0	0	**0**	0	0	0	0	0	0	0	0	0	0	0	
Ti + Heat One, CentCast+HIP+ SHTA: 1.8 - 2.0mm	1	2	0	0	2	**2**	2	0	0	**2**	4	0	4	2	0	2	0	0	1	1	0	
Ti + Heat One, CentCast+HIP+SHTA: 8 - 10mm	1	1	**0**	0	**1**	**1**	**1**	0	0	**1**	**1**	**0**	**1**	**4**	**0**	**4**	**0**	**0**	**1**	**1**	0	
Ti+ Heat One, CentCast+HIP+SHTA:20 - 22mm	1	1	**0**	0	**1**	**1**	**1**	0	0	**1**	**1**	**0**	**1**	**2**	**0**	**2**	**0**	**0**	**1**	**1**	0	
Ti + Heat One, CentCast+HIP+SHTA: 25 - 35mm	1	2	0	0	2	**2**	2	0	0	**2**	4	0	4	4	0	4	**6**	**6**	1	1	2	
Ti + Heat Two, CentCast+HIP+SHTA: 1.8 - 2.0mm	1	2	0	0	1	**1**	1	0	0	**1**	0	0	0	0	0	0	**0**	**0**	0	0	0	
Ti + Heat Two, CentCast+HIP+SHTA: 8 - 10mm	1	1	**0**	0	**1**	**0**	**1**	0	0	**0**	**0**	**0**	**0**	**0**	**0**	**0**	**0**	**0**	**0**	**0**	0	
Ti + Heat Two, CentCast+HIP+SHTA: 20 - 22mm	1	1	**0**	0	**1**	**0**	**1**	0	0	**0**	**0**	**0**	**0**	**0**	**0**	**0**	**0**	**0**	**0**	**0**	0	
Ti + Heat Two, CentCast+HIP+SHTA: 25 - 35mm	1	2	0	0	1	**1**	1	0	0	**1**	0	0	0	0	0	0	**0**	**0**	0	0	0	
Ti + Heat Three, GravCast+HIP+SHTA: 1.8 - 2.0mm	1	2	0	0	2	**2**	2	0	0	**2**	2	0	0	2	0	2	0	0	1	1	0	
Ti+ Heat Three, GravCast+HIP+SHTA: 8 - 10mm	1	2	0	0	**1**	**1**	**1**	0	0	**1**	**0**	**0**	**0**	**4**	**0**	**4**	**0**	**0**	**1**	**1**	0	
Ti+ Heat Three, GravCast+HIP+SHTA: 20 - 22mm	1	2	0	0	**1**	**1**	**1**	0	0	**1**	**0**	**0**	**0**	**2**	**0**	**2**	**0**	**0**	**1**	**1**	0	
Ti+ Heat Three, GravCast+HIP+SHTA: 25 - 35mm	1	2	0	0	2	**2**	2	0	0	**2**	2	0	0	4	0	4	**6**	**6**	1	1	2	
Ti + Heat One, CentCast: 25 - 35mm:HIP+SHTA + Repair + SHTA	1	2	**0**	**0**	**2**	**2**	**2**	**0**	**0**	**2**	**4**	**0**	**0**	**4**	**0**	**4**	**0**	**0**	**1**	**1**	**0**	
Ti + Heat One, CentCast: 25 - 35mm:HIP+SHTA + [Repair + SHTA] x4	1	2	0	**0**	2	**2**	2	**0**	**0**	**2**	4	0	**0**	4	0	4	**0**	**0**	1	1	2	
Ti 6242S Sheet: 2mm	0	2	1	2	2	**0**	0	2	2	**0**	0	4	0	4	0	4	0	0	1	0	0	1
Ti 6242S Sheet: 4mm	0	2	1	2	2	**0**	0	2	2	**0**	0	4	0	4	4	0	0	0	1	0	0	1
Ti+ Heat Seven:Sheet: 2.0mm	0	2	**1**	**0**	**2**	**2**	**2**	**0**	**0**	**2**	**4**	**0**	**0**	**4**	**0**	**4**	0	0	**1**	**1**	**0**	
Ti+ Heat Seven: Sheet: 4.0mm	0	2	1	**0**	**2**	**2**	**2**	**0**	**0**	**2**	4	0	**0**	4	0	4	0	0	1	1	**0**	
Ti+ Weld wire: 2.0mm	0	1	0	0	0	**0**	0	0	0	**0**	0	0	0	0	0	0	0	0	0	0	0	
Ti+ / Ti+ welds sheet to sheet; 2mm S/R	1	2	0	0	2	**2**	2	0	0	**2**	4	0	0	4	0	4	0	0	1	1	0	
Ti+ / Ti+ welds sheet to sheet; 4mm, S/R	1	2	0	0	2	**2**	2	0	0	**2**	4	0	0	4	0	4	0	0	1	1	0	
Ti+ sheet / Ti+ cast 2mm [Preferred casting method]	1	2	0	0	2	**2**	2	0	0	**2**	4	0	0	4	0	6	0	0	1	1	0	
Ti 6242S / Ti+ welds: 2mm, S/R	1	2	0	2	2	**0**	0	2	2	**0**	0	4	0	4	4	0	0	0	1	1	0	
Ti 6242S / Ti+ welds: 4.0mm S/R	1	2	0	2	2	**0**	0	2	2	**0**	0	4	0	4	4	0	0	0	1	1	0	
																						test total
	27	**57**	7	14	50	**32**	34	14	14	**32**	46	24	14	86	28	60	18	18	24	22	10	**540**

Figure 1 Initial GOTA testing plan

This plan was revised during the project due to concerns that arose with the post exposure ductility of the Ti-834 cast material. The testing became more focused on the effect of various exposure times on the tensile ductility of the centrifugally cast Ti-834 material.

To create a benchmark for the testing Ti-6242S was tested in its cast and sheet forms:

- Cast specimens were taken from stock with diameters/thicknesses of 1.8-2mm, 13mm, 20-22mm and 25-35mm.
- Sheet specimens were tested at thicknesses of 2mm and 4mm.

Ti-834 was tested in a number forms:

- Forged condition; where specimens were taken from the circumferential direction of rolled rings.
- Centrifugally cast specimens were taken from stock with diameters/thicknesses of 1.8-2mm, 13mm, 20-22mm and 25-35mm.
- Gravity cast specimens were taken from stock with diameters/thicknesses of 1.8-2mm, 13mm, 20-22mm and 25-35mm.
- Sheet specimens were tested at thicknesses of 2mm and 4mm.
- Welded sheet specimens were tested at thicknesses of 2mm and 4mm.
- Centrifugally cast material was also tested after undergoing a hydrogen anneal + vacuum degas (HDH) process intended to refine the microstructure. Specimens were taken from stock with diameters of 13mm and 25-35mm.

2.3 Exposure

Exposures were performed in air in a Carbolite CWF 1200 box furnace; these were followed in all instances by air cooling. All Ti-6242S specimens were exposed at 450^{o}C, while all Ti-834 specimens were exposed at 500^{o}C. Exposure times of 25, 100, 200, 500 and 1000 hours were employed during the project.

2.4 Specimens

Flat plate specimens conforming to test piece design RLH6009 were manufactured for the purpose of tensile and LCF testing of sheet products. The test-piece design is illustrated in Figure 2. Cylindrical tensile specimens conforming to test piece design TIMET R6 were manufactured for the purpose of tensile testing all cast and forged products. The test-piece design is illustrated in Figure 3. Cylindrical low cycle fatigue specimens conforming to test piece design RLH10113 were manufactured for the purpose of LCF testing of all 25mm diameter cast product and all forged ring specimens. The test-piece design is illustrated in Figure 4. Cylindrical low cycle fatigue specimens conforming to test piece design RLH8001 were manufactured for the purpose of LCF testing of all 13mm diameter cast product specimens. The test-piece design is illustrated in Figure 5.

Cylindrical creep specimens conforming to test piece design RLH10259 were manufactured for the purpose of all creep testing. The test-piece design is illustrated in Figure 6.

Square test pieces with corner cracks conforming to test piece design RLH10042 were manufactured for the purpose of all 25mm fatigue crack propagation testing. The test-piece design is illustrated in Figure 7.

Square test pieces with corner cracks conforming to test piece design RLH5325 were manufactured for the purpose of all 13mm fatigue crack propagation testing. The test-piece design is illustrated in Figure 8.

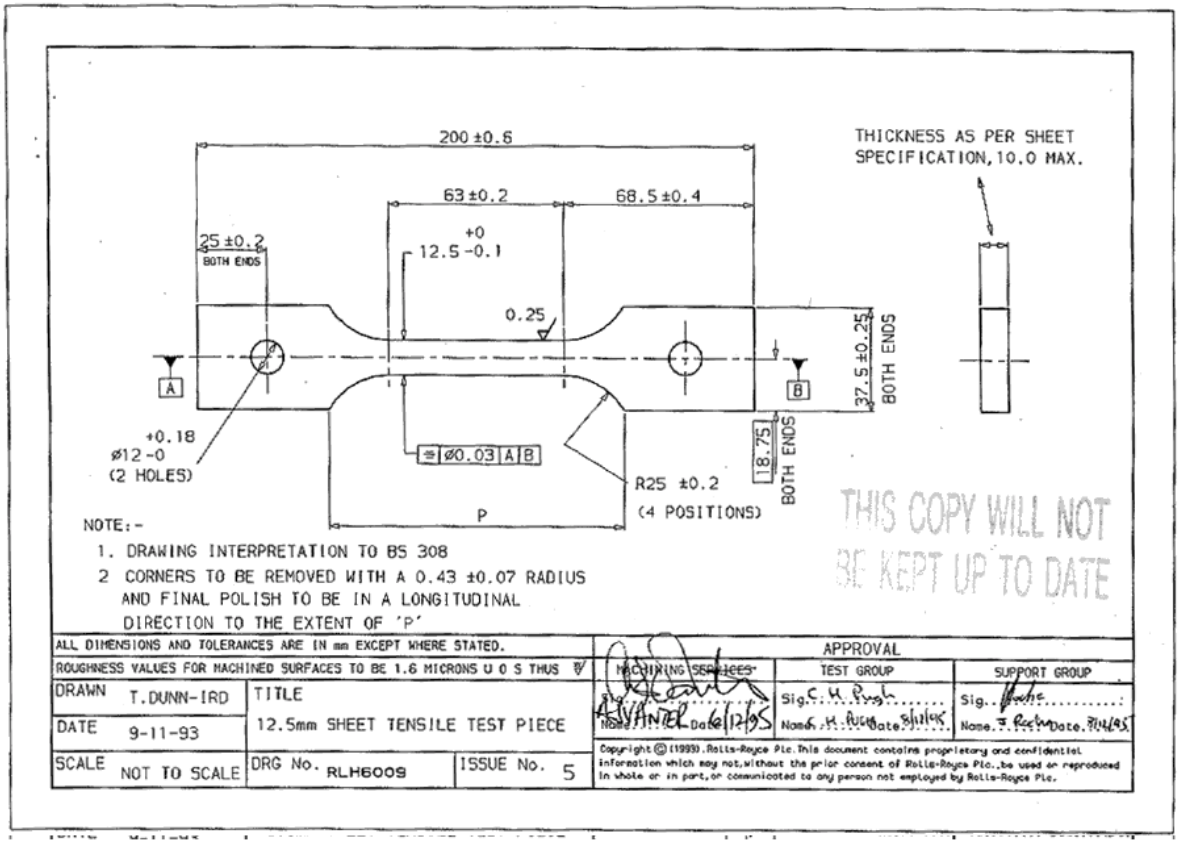

Figure 2 Specimen design RLH6009 employed during this project.

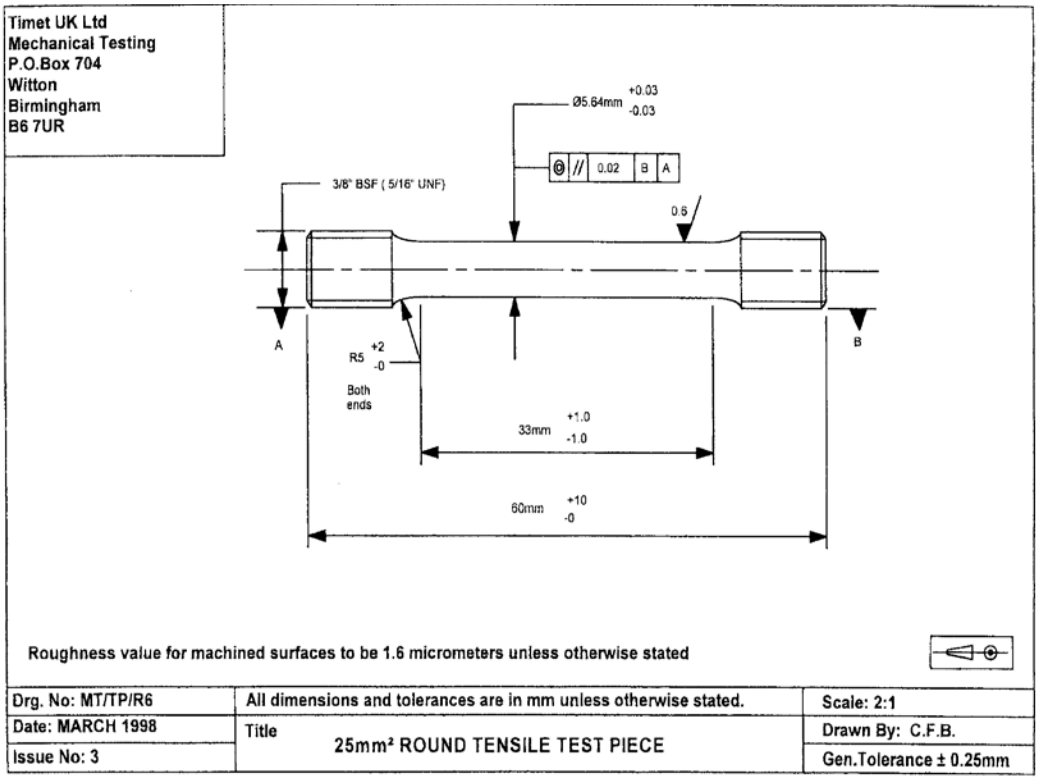

Figure 3 Specimen design TIMET R6 employed during this project.

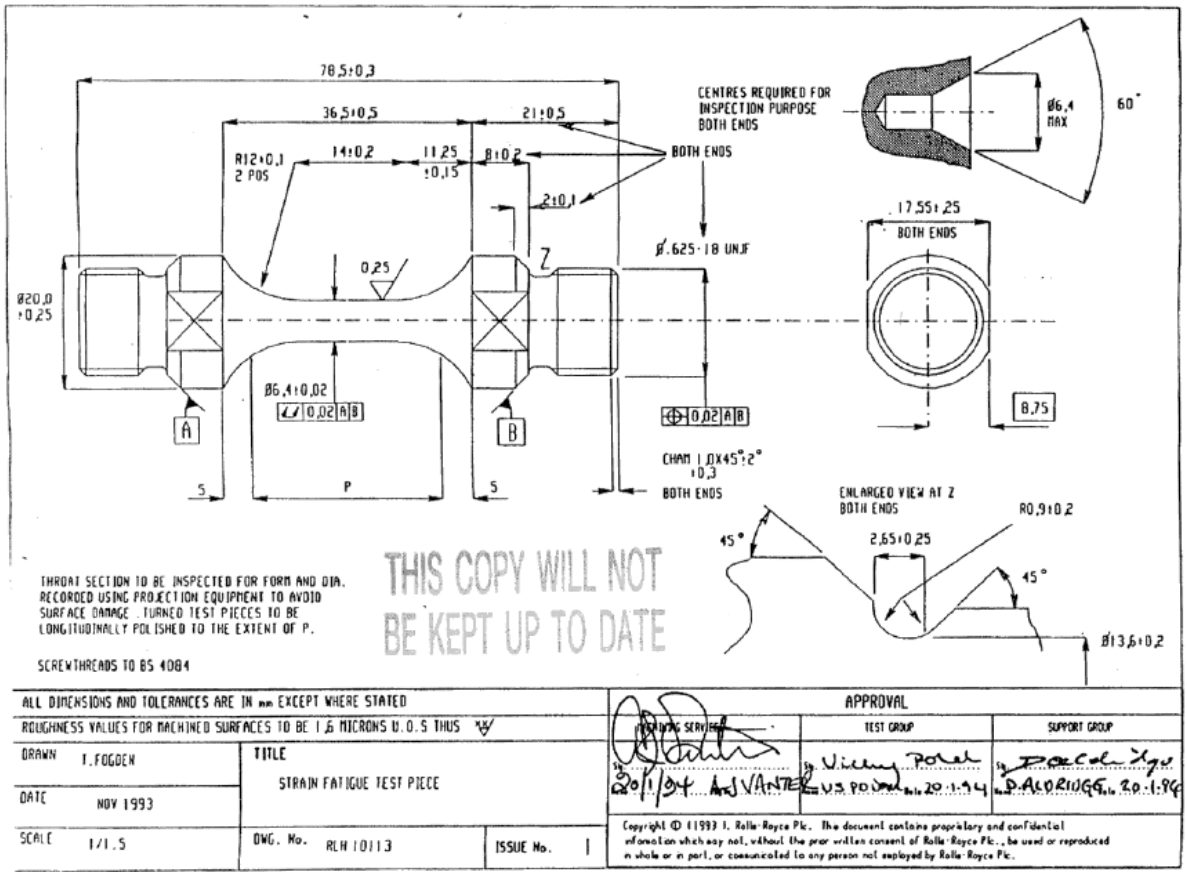

Figure 4 Specimen design RLH10113 employed during this project.

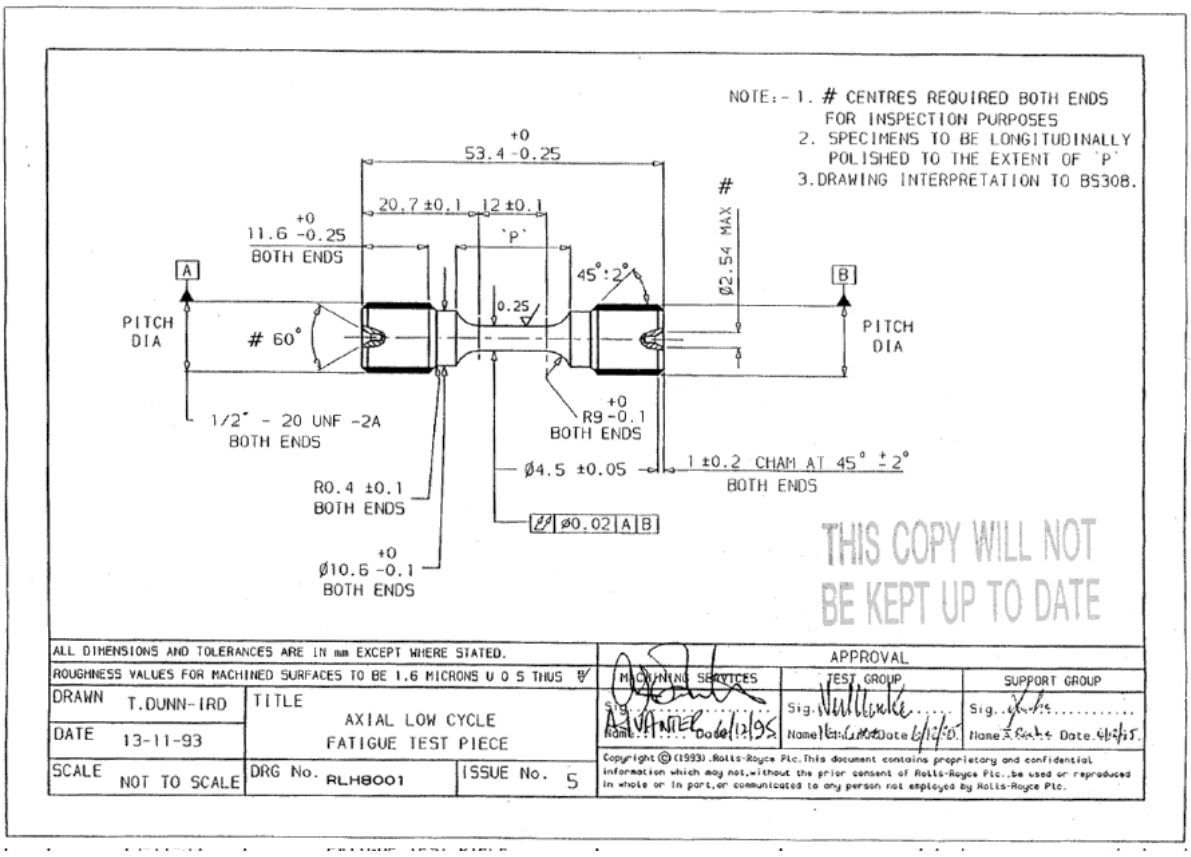

Figure 5 Specimen design RLH8001 employed during this project.

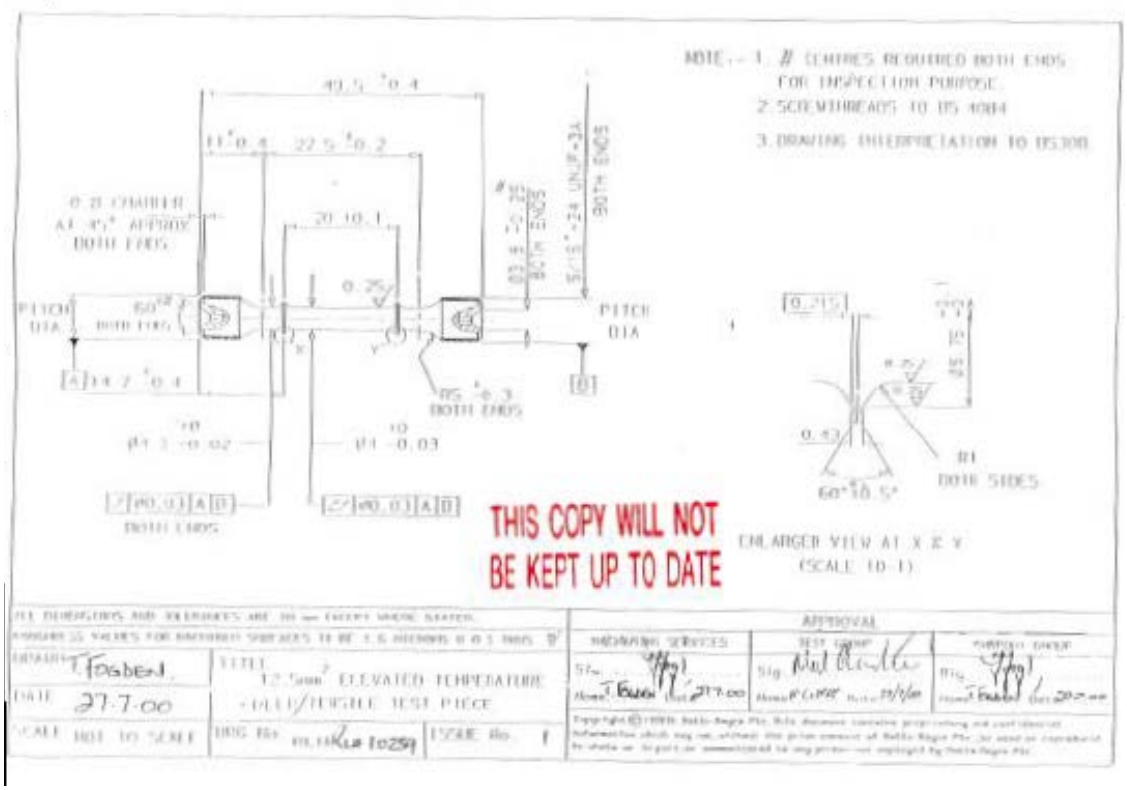

Figure 6 Specimen design RLH10259 employed during this project.

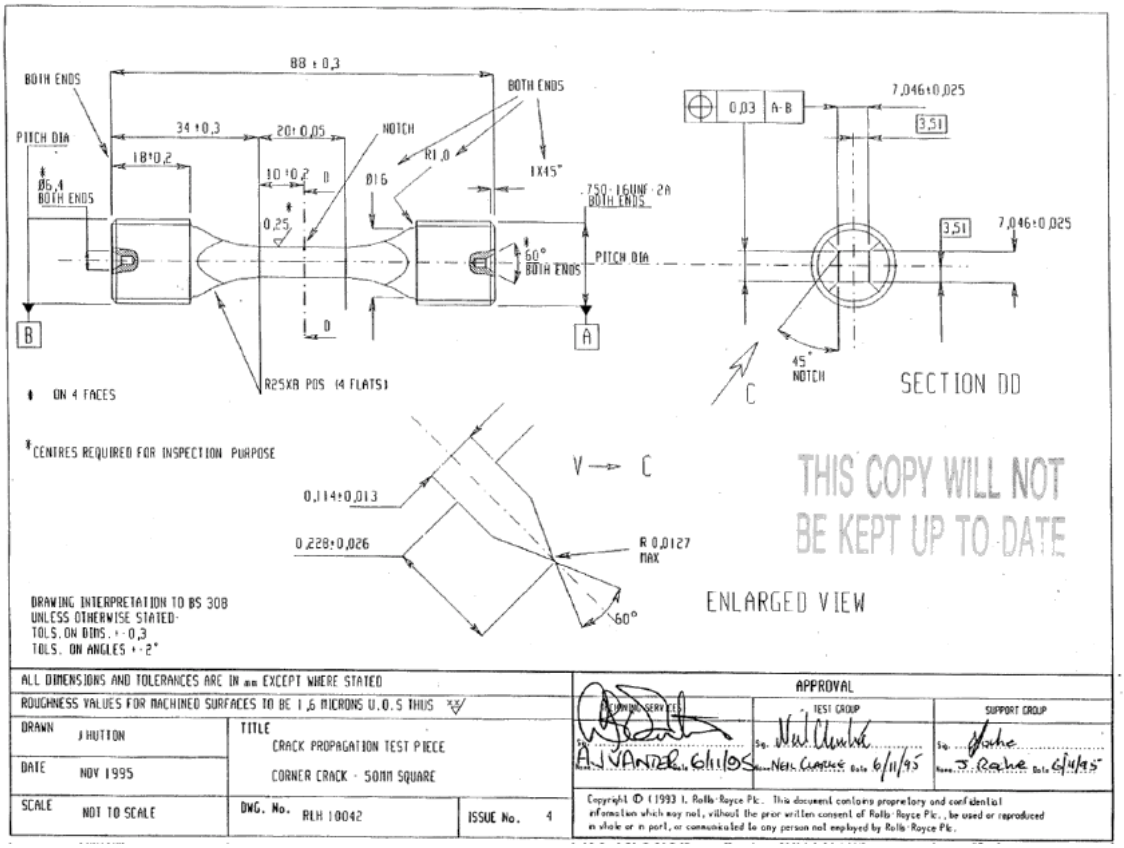

Figure 7 Specimen design RLH10042 employed during this project.

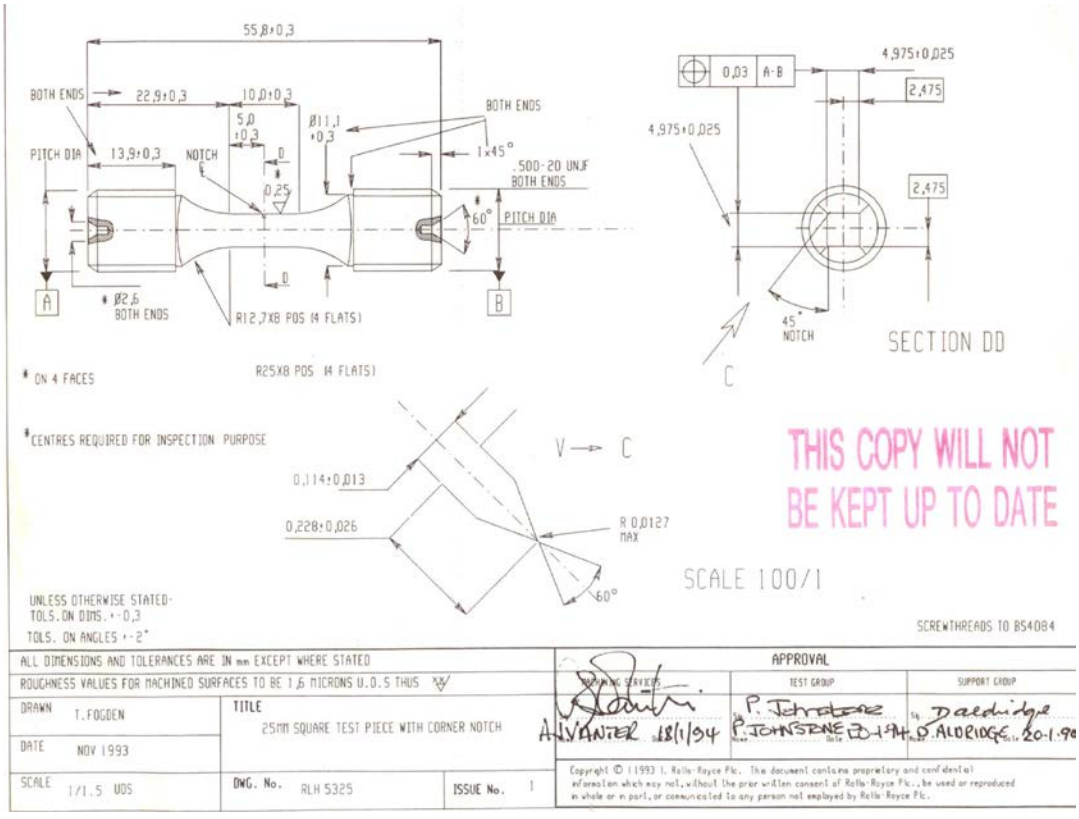

Figure 8 Specimen design RLH5325 employed during this project.

2.5 Test Methods

All tensile tests within this project were carried- out in accordance with the in-house standard test operating procedure: SMaRT_QS 5.4d(2) STOP_TMM: Test Method and Data Analysis for Tensile Testing of Metallic Materials. This document adheres to the standards listed in appendix a.

All force controlled LCF tests within this contract were carried-out in accordance with the in-house standard test operating procedure: SMaRT_QS5.4d (1) STOP Force Controlled Fatigue Testing. This document adheres to the standards listed in appendix b.

All strain controlled LCF tests within this contract were carried-out in accordance with the in-house standard test operating procedure: SMaRT_QS5.4d(3) STOP_SLCF Strain Controlled Low Cycle Fatigue Test Procedures. This document adheres to the standards listed in appendix c.

All creep tests within this project were carried- out in accordance with the in-house standard test operating procedure: SMaRT_QS5.4d(5) STOP_CLC Constant Load Creep Test Procedure. This document adheres to the standards listed in appendix d.

All fatigue crack propagation tests within this project were carried- out in accordance with the in-house standard test operating procedure: SMaRT_QS 5.4d(4) STOP_CCG Fatigue crack growth in metallic materials - corner crack geometry. Appendix e

2.6 Test Conditions

Tensile testing of Ti-6242S was performed at room temperature and 450^{o}C. Tensile testing of all Ti-834 products was performed at room temperature and 500^{o}C. Dual strain rates of 0.00005^{s-1} up until 2% strain and 1mm/min thereafter were employed for the tests.

Load control LCF testing was performed at room and elevated temperatures (450^{o}C Ti-6242S, 500^{o}C Ti-834). Room temperature tests were performed at loads of 950MPa and 750MPa, at elevated temperature loads of 750MPa and 650MPa were employed. An R ratio of 0.01 was utilised for all tests.

Strain control LCF testing was performed at room and elevated temperatures (450^{o}C Ti-6242S, 500^{o}C Ti-834). Room temperature tests were performed at maximum strains of 1.0% and 0.55% on all cast products, at elevated temperature maximum strains of 1.2% and 0.65% were employed on all cast products. Room temperature tests were performed at maximum strains of 1.5% and 0.8% on all

forged products, at elevated temperature maximum strains of 1.5% and 0.9% were employed on all forged products. An R ratio of 0.01 was applied for all tests.

Creep testing was performed at elevated temperatures of 450^{o}C for Ti-6242S and 500^{o}C for Ti-834 products. Tests were performed at levels between 450MPa and 625MPa during this project.

Fatigue crack propagation tests were performed in load control at room temperature. Room temperature tests were performed at a peak stress of 520MPa, elevated temperature tests were performed at a peak stress of 315MPa. A triangular waveform was used for all tests.

3. Results

The microstructures of the materials investigated are illustrated in this section:

The centrifugally cast Ti-6242S alloy displayed an equiaxed lamellar microstructure (Figure 9) with an average prior β grain size of approx. 730µm in diameter. The β grains are surrounded by a continuous layer of grain boundary alpha several microns in width.

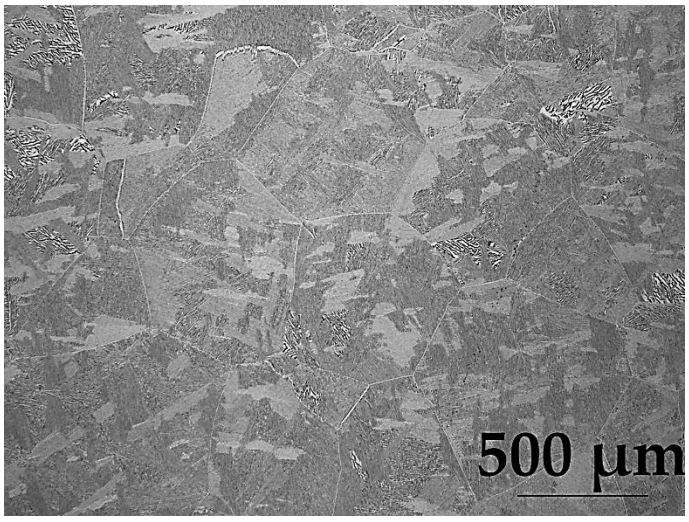

Figure 9 Ti-6242S centrifugally cast alloy

The centrifugally cast Ti-834 alloy also displayed an equiaxed lamellar microstructure (Figure 10) with an average prior β grain size of approximately 850µm in diameter. The β grains are once again surrounded by a constant layer of grain boundary alpha several microns in width.

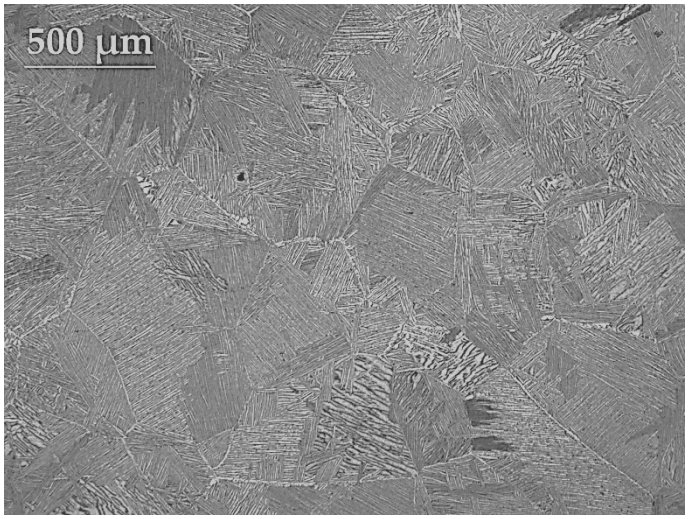

Figure 10 Ti-834 centrifugally cast alloy

The 13mm HDH processed centrifugally cast Ti-834 alloy displayed a finer equiaxed lamellar microstructure (Figure 11) when compared to the base material, with an average prior β grain size of approximately 435µm in diameter. The internal structure of these grains illustrated in figure 11b contrasted with the base material; displaying a Widmanstatten type structure compared to the coarse alpha lath structure of the base alloy. The β grains are once again surrounded by a continuous layer of grain boundary alpha several microns in width.

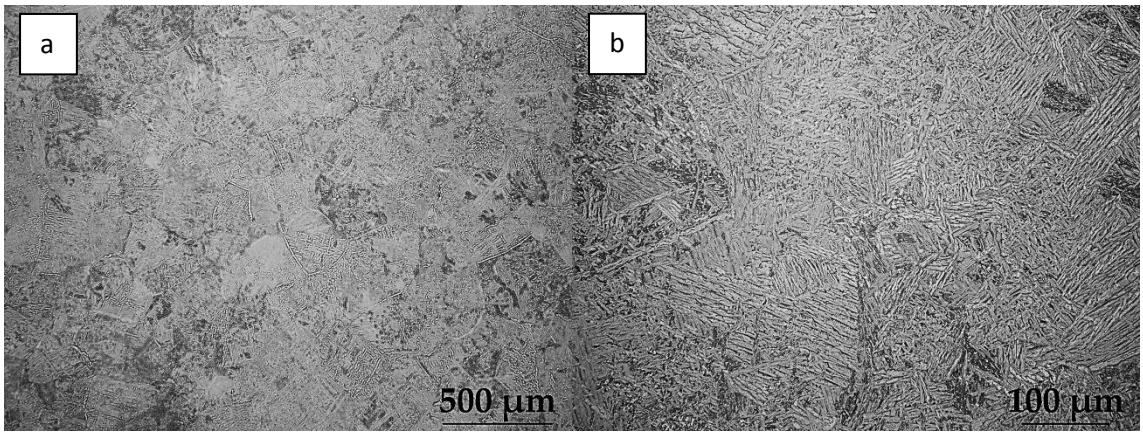

Figure 11 Ti-834 13mm hydrogenated centrifugally cast alloy

The 23mm HDH centrifugally cast Ti834 alloy displayed a coarser equiaxed lamellar microstructure (Figure 12) when compared to the 13mm material, with an average prior β grain size of approximately 700µm in diameter. The internal structure of these grains illustrated in figure 12b also displayed a Widmanstatten type structure. The β grains are once again surrounded by a continuous layer of grain boundary alpha several microns in width.

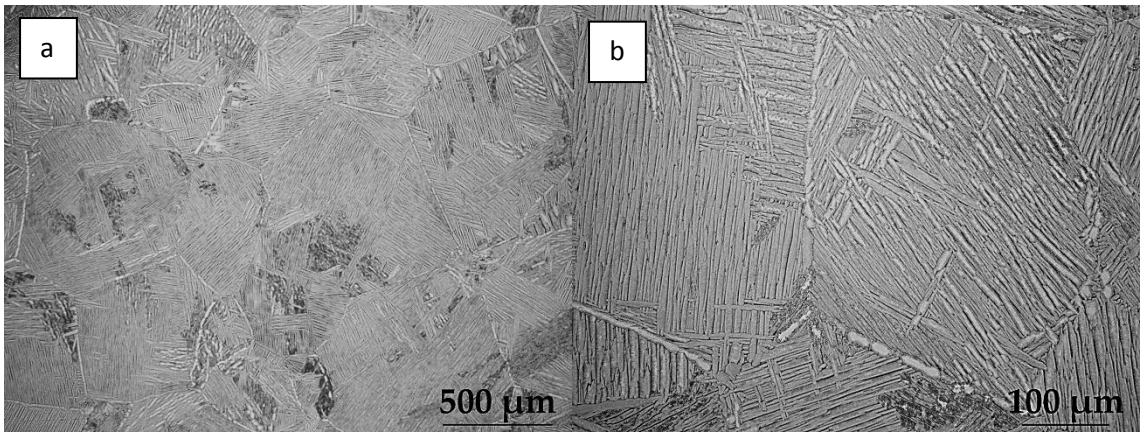

Figure 12 Ti-834 13mm hydrogenated centrifugally cast alloy

The gravity cast Ti-834 alloy as expected also displayed an equiaxed lamellar microstructure (Figure 13), the material had a very large grain size with an average prior β grain size approximately 2176µm in diameter. The β grains are once again surrounded by a layer of grain boundary α.

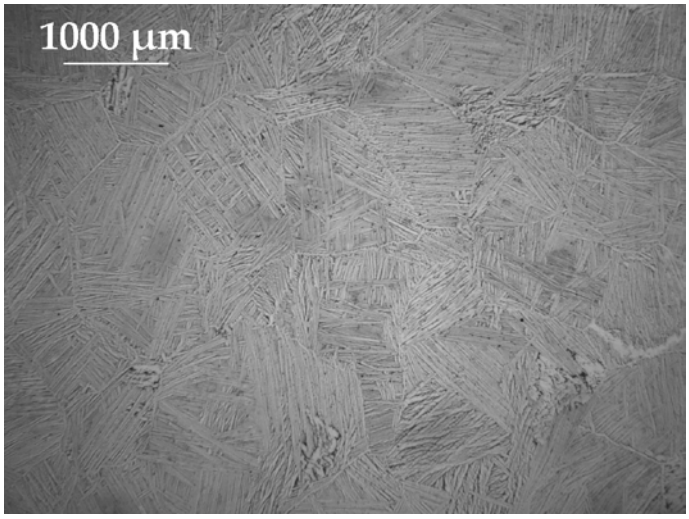

Figure 13 Ti-834 gravity cast alloy

The forged Ti-834 alloy displayed an equiaxed bimodal microstructure (Figure 14) with an average primary alpha grain size approximately 20µm in diameter.

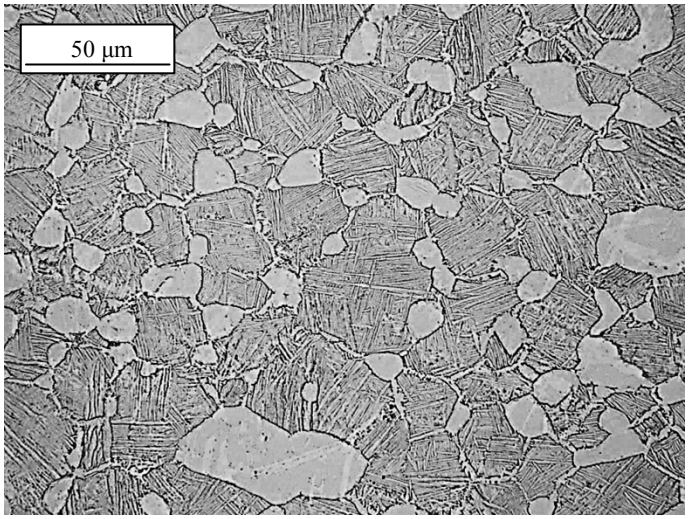

Figure 14 Ti-834 forged alloy

The Ti-6242S 2mm sheet alloy displayed a duplex microstructure (Figure 15) with an average primary alpha grain size approximately 15µm in diameter.

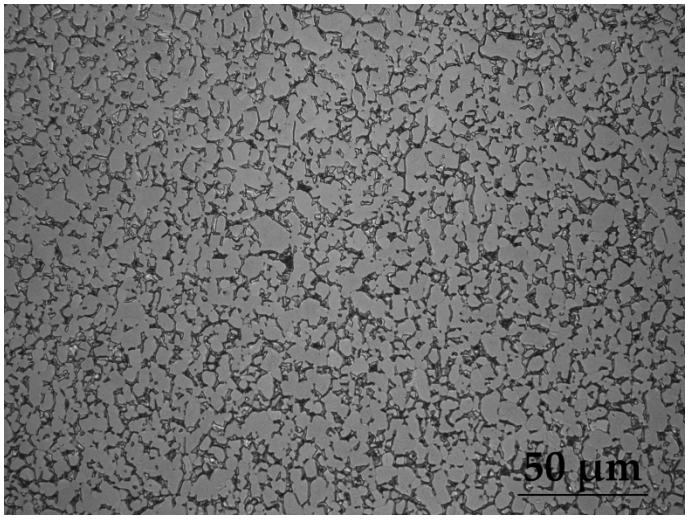

Figure 15 Ti-6242 2mm sheet

The Ti-6242S 4mm sheet alloy displayed a duplex microstructure (Figure 16) with an average primary alpha grain size of approximately 16µm in diameter.

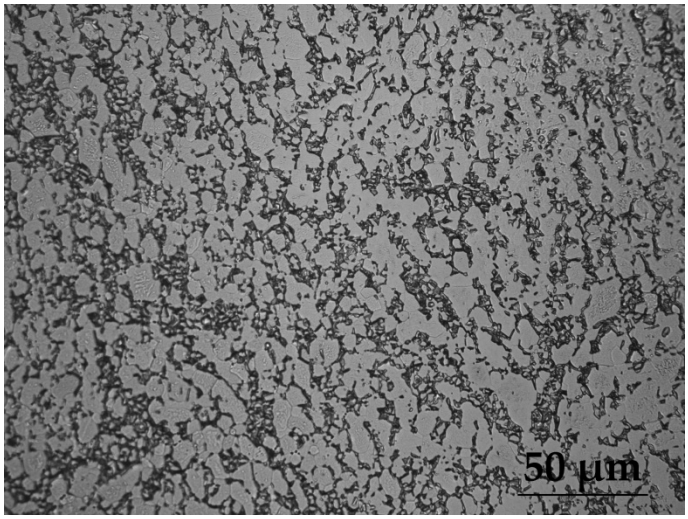

Figure 16 Ti-6242 4mm sheet

The Ti-834 2mm sheet alloy displayed ae bimodal microstructure (Figure 17) with an average primary alpha grain size of approximately 18µm in diameter.

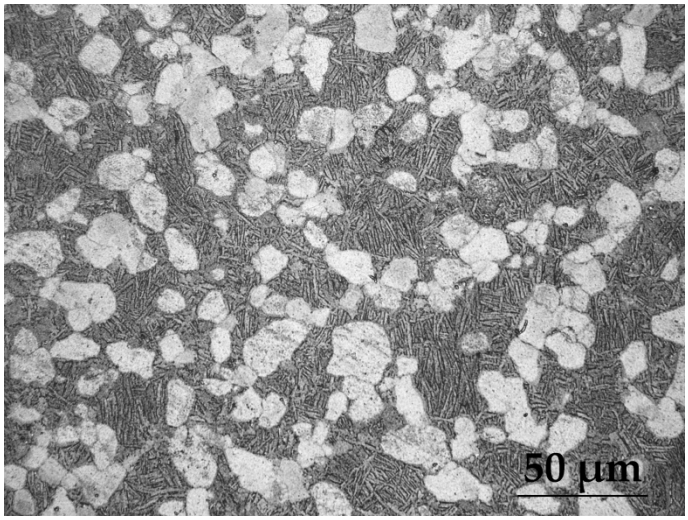

Figure 17 Ti-834 2mm sheet

The Ti-834 4mm sheet alloy displayed a bimodal microstructure (Figure 18) with an average primary alpha grain size of approximately 20µm in diameter.

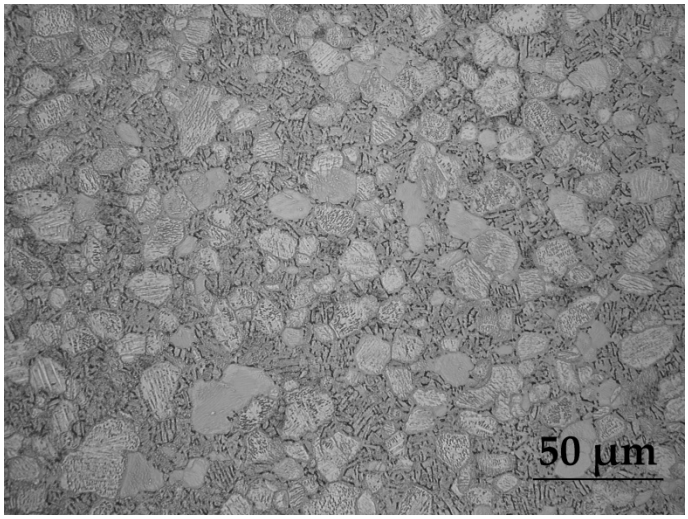

Figure 18 Ti-834 4mm sheet

3.1 Ti-6242S Centrifugally Cast

The tensile results for the Ti-6242S centrifugally cast alloy are displayed in table 1, the alloy was found to have reasonably high strength and ductility at room and elevated temperature.

Table 1 Tensile results for Ti-6242S cast products

STS NO.	Material	Exposure Time, @450°C (hrs)	Oxide Retained	Test Temp (°C)
2013-9162	Ti6242S CC 13mm	none	N/A	20
2013-9164	Ti6242S CC 13mm	none	N/A	20
2013-9163	Ti6242S CC 13mm	none	N/A	450
2013-9438	Ti6242S CC 13mm	1000	Y	450
2013-9151	Ti6242S CC 25-35mm	none	N/A	20
2013-9152	Ti6242S CC 25-35mm	none	N/A	20
2013-9154	Ti6242S CC 25-35mm	none	N/A	450
2013-9156	Ti6242S CC 25-35mm	none	N/A	450
2013-9434	Ti6242S CC 25-35mm	1000	Y	450
2013-9435	Ti6242S CC 25-35mm	1000	Y	450
2013-9436	Ti6242S CC 25-35mm	1000	Y	20
2013-9437	Ti6242S CC 25-35mm	1000	Y	20

The room temperature LCF results for the Ti-6242S 13mm centrifugally cast alloy are displayed in table 2.

Table 2 Room temperature LCF results for Ti-6242S 13mm cast products

STS NO.	Material	Exposure Time, @450°C (hrs)	Test Temp (°C)	R Ratio	Peak Strain (%)
STS2014_9752	Ti 6242S 13mm	None	20	0	1
STS2014_9753	Ti 6242S 13mm	None	20	0	0.47
STS2014_9754	Ti 6242S 13mm	None	20	0	1
STS2014_9755	Ti 6242S 13mm	None	20	0	0.55
STS2014_9756	Ti 6242S 13mm	None	20	0	1
STS2014_9757	Ti 6242S 13mm	None	20	0	0.55
STS2014_9758	Ti 6242S 13mm	None	20	0	1

The LCF results at 450°C for the Ti-6242S 13mm centrifugally cast alloy are displayed in table 3.

Table 3 Elevated temperature LCF results for Ti-6242S 13mm cast products

STS NO.	Material	Exposure Time, @450°C (hrs)	Test Temp (°C)	R Ratio	Peak Strain (%)
STS2014_9759	Ti 6242S 13mm	None	450	0	1.2
STS2014_9760	Ti 6242S 13mm	None	450	0	0.65
STS2014_9764	Ti 6242S 13mm	None	450	0	1.2
STS2014-9765	Ti 6242S 13mm	None	450	0	1.2

The room temperature LCF results for the Ti-6242S 25mm centrifugally cast alloy are displayed in table 4.

Table 4 Room temperature LCF results for Ti-6242S 25-35mm cast products

STS NO.	Material	Exposure Time, @450°C (hrs)	Test Temp (°C)	R Ratio	Peak Strain (%)
STS2013-9365	Ti 6242S 25-35mm	None	20	0	0.47
STS2013-9366	Ti 6242S 25-35mm	None	20	0	0.47
STS2013-9368	Ti 6242S 25-35mm	None	20	0	1
STS2013-9369	Ti 6242S 25-35mm	None	20	0	0.47
STS2013-9370	Ti 6242S 25-35mm	None	20	0	1
STS2013-9374	Ti 6242S 25-35mm	None	20	0	1

The LCF results at 450°C for the Ti-6242S 25mm centrifugally cast alloy are displayed in table 5.

Table 5 Elevated temperature LCF results for Ti-6242S 25-35mm cast products

STS NO.	Material	Exposure Time, @450°C (hrs)	Test Temp (°C)	R Ratio	Peak Strain (%)
STS2013-9375	Ti 6242S 25-35mm	None	450	0	1.2
STS2013-9376	Ti 6242S 25-35mm	None	450	0	1.2
STS2013-9377	Ti 6242S 25-35mm	None	450	0	0.65
STS2013-9373	Ti 6242S 25-35mm	None	450	0	0.65

The creep results for the Ti-6242S 25mm centrifugally cast alloy are displayed in table 6.

Table 6 Creep results for Ti-6242S 25-35mm cast products

STS NO.	Material	Exposure Time, @450°C (hrs)	Test Temp (°C)	Stress (MPa)
2013-9378	Ti6242S CC 25-35mm	none	450	600
2013-9379	Ti6242S CC 25-35mm	none	450	600
2013-9380	Ti6242S CC 25-35mm	none	450	600
2013-9382	Ti6242S CC 25-35mm	none	450	575

The data recorded from FCP tests for Ti-6242S 13mm centrifugally cast alloy are displayed in table 7.

Table 7 FCP results for Ti-6242S cast 13mm products

STS NO.	Material	Exposure Time, @450°C (hrs)	Test Temp (°C)	Stress (MPa)
2014-9506	Ti6242S CC 13mm	none	20	520

The data recorded from FCP tests for Ti-6242S 25mm centrifugally cast alloy are displayed in table 8.

Table 8 FCP results for Ti-6242S cast 25mm products

STS NO.	Material	Exposure Time, @450°C (hrs)	Test Temp (°C)	Stress (MPa)
2014-9507	Ti6242S CC 25mm	none	20	520

a. Ti-6242S Sheet

The tensile results for the Ti-6242S sheet alloy are displayed in this section.

Table 9, details the tensile results for the 2mm sheet at room temperature and 450°C, together with results of testing under the same conditions after exposure at 450°C for 1000 hours.

Table 9 Tensile results for Ti-6242S 2mm sheet products

STS NO.	Material	Exposure Time, @450°C (hrs)	Oxide Retained	Test Temp (°C)
2013-6746	Ti6242S -2mm	1000	Y	20
2013-6747	Ti6242S -2mm	1000	Y	20
2013-6748	Ti6242S -2mm	none	N/A	20
2013-6749	Ti6242S -2mm	none	N/A	20
2013-6750	Ti6242S -2mm	none	N/A	450
2013-6757	Ti6242S -2mm	1000	Y	450
2013-6758	Ti6242S -2mm	1000	Y	20
2013-6759	Ti6242S -2mm	1000	Y	20
2013-6760	Ti6242S -2mm	none	N/A	20

2013-6761	Ti6242S -2mm	none	N/A	20
2013-6762	Ti6242S -2mm	none	N/A	450
2013-6763	Ti6242S -2mm	1000	Y	450

The tensile results at room and elevated temperature for the 4mm sheet variant are shown in table 10, together with further tensile tests after exposure at 450°C for 100 hours.

Table 10 Tensile results for Ti-6242S 4mm sheet products

STS NO.	Material	Exposure Time, @450°C (hrs)	Oxide Retained	Test Temp (°C)
2015-12371	Ti6242S -4mm	100	Y	20
2015-12372	Ti6242S -4mm	None	N/A	20
2015-12377	Ti6242S -4mm	None	N/A	450
2015-12379	Ti6242S -4mm	None	N/A	20
2015-12380	Ti6242S -4mm	100	Y	20
2015-12383	Ti6242S -4mm	None	N/A	20

The room temperature LCF results for the Ti-6242S 2mm sheet alloy are displayed in table 11. Lower stress levels of 750MPa resulted in long lives with both specimens.

Table 11 Room temperature LCF results for Ti-6242S 2mm sheet products

STS NO.	Material	Exposure Time, @450°C (hrs)	Test Temp (°C)	R Ratio	Stress (MPa)
2013-6751	Ti6242S -2mm	None	20	0.01	950
2013-6756	Ti6242S -2mm	None	20	0.01	750
2013-6765	Ti6242S -2mm	None	20	0.01	950
2013-6766	Ti6242S -2mm	None	20	0.01	750

The elevated temperature LCF results for the Ti-6242S 2mm sheet alloy are illustrated in table 12.

Table 12 Elevated temperature LCF results for Ti-6242S 2mm sheet products

STS NO.	Material	Exposure Time, @450°C (hrs)	Test Temp (°C)	R Ratio	Stress (MPa)
2013-6754	Ti6242S -2mm	None	450	0.01	750
2013-6755	Ti6242S -2mm	None	450	0.01	750

2014-10785	Ti6242S -2mm	None	450	0.01	650
2014-10786	Ti6242S -2mm	None	450	0.01	650
2014-10787	Ti6242S -2mm	None	450	0.01	600

Similar LCF results to the 2mm sheet were seen at room temperature for the Ti-6242S 4mm sheet alloy displayed in table 13.

Table 13 Room temperature LCF results for Ti-6242S 4mm sheet products

STS NO.	Material	Exposure Time, @450°C (hrs)	Test Temp (°C)	R Ratio	Stress (MPa)
2015-12378	Ti6242S -4mm	None	20	0.01	950
2015-12364	Ti6242S -4mm	None	20	0.01	950
2015-12374	Ti6242S -4mm	None	20	0.01	750
2015-12563	Ti6242S -4mm	None	20	0.01	750

The elevated temperature LCF results for the Ti-6242S 4mm sheet alloy are shown in table 14.

Table 14 Elevated temperature LCF results for Ti-6242S 4mm sheet products

STS NO.	Material	Exposure Time, @450°C (hrs)	Test Temp (°C)	R Ratio	Stress (MPa)
2015-12565	Ti6242S -4mm	None	450	0.01	650
2015-12376	Ti6242S -4mm	None	450	0.01	650
2015-12566	Ti6242S -4mm	None	450	0.01	750
2015-12375	Ti6242S -4mm	None	450	0.01	750

b. Ti 834 Forged Ring

The room temperature tensile results for the Ti-834 forged material can be seen in table 15. Exposure times were modified to between 25 and 500 hours for the forged material.

Table 15 Room temperature tensile results Ti-834 forged ring

STS NO.	Material	Exposure Time, @500°C (hrs)	Oxide Retained	Test Temp (°C)
2014-10924	Ti834 Ring	None	N/A	20

2014-10927	Ti834 Ring	None	N/A	20
2014-10928	Ti834 Ring	None	N/A	20
*MT6671(F6)	Ti834 Ring	None	N/A	20
*MT6672(F6)	Ti834 Ring	None	N/A	20
2014-10932	Ti834 Ring	25	Y	20
2014-10935	Ti834 Ring	100	Y	20
*MT6680(G6)	Ti834 Ring	100	Y	20
*MT6681(G6)	Ti834 Ring	100	Y	20
2014-10938	Ti834 Ring	200	Y	20
2014-10936	Ti834 Ring	500	Y	20
2014-10940	Ti834 Ring	25	N	20
2014-10943	Ti834 Ring	100	N	20
2014-10947	Ti834 Ring	200	N	20
2014-10944	Ti834 Ring	500	N	20

*Tests performed at TIMET

The elevated temperature tensile results for the Ti-834 forged material are illustrated in table 16. Exposure times were again modified to between 25 and 500 hours.

Table 16 Elevated temperature tensile results Ti-834 forged ring

STS NO.	Material	Exposure Time, @ 500°C (hrs)	Oxide Retained	Test Temp (°C)
2014-10929	Ti834 Ring	None	N/A	500
2014-10930	Ti834 Ring	None	N/A	500
2014-10931	Ti834 Ring	None	N/A	500
*MT6693 (H6)	Ti834 Ring	None	N/A	500
*MT6694 (H6)	Ti834 Ring	None	N/A	500
2014-10933	Ti834 Ring	25	Y	500
2014-10934	Ti834 Ring	100	Y	500
2014-10939	Ti834 Ring	200	Y	500
2014-10937	Ti834 Ring	500	Y	500
2014-10941	Ti834 Ring	25	N	500
2014-11162	Ti834 Ring	200	N	500
2014-10945	Ti834 Ring	500	N	500

*Tests performed at TIMET

The room temperature LCF results for the Ti-834 forged ring material are shown in table 17.

Table 17 Room temperature LCF results Ti-834 forged ring

STS NO.	Material	Exposure Time, @500(hrs)	Oxide Retained	Test Temp (^{o}C)	R Ratio	Peak Strain (%)
2014-10688	Ti834 Ring	None	N/A	20	0	1.5
2014-10689	Ti834 Ring	None	N/A	20	0	1.4
2014-10690	Ti834 Ring	None	N/A	20	0	1.5
2014-10691	Ti834 Ring	None	N/A	20	0	0.8
2014-10692	Ti834 Ring	None	N/A	20	0	0.8
2014-10693	Ti834 Ring	None	N/A	20	0	0.8
2014-10701	Ti834 Ring	100	Y	20	0	1.5
2014-10702	Ti834 Ring	100	Y	20	0	1.5
2015-12416	Ti834 Ring	100	Y	20	0	1.5
2015-12412	Ti834 Ring	100	Y	20	0	0.8
2015-12413	Ti834 Ring	100	Y	20	0	0.8
2015-12414	Ti834 Ring	100	Y	20	0	0.8
2014-10680	Ti834 Ring	700	Y	20	0	0.8
2014-10687	Ti834 Ring	700	Y	20	0	0.8
2014-10686	Ti834 Ring	700	Y	20	0	0.8
2014-10681	Ti834 Ring	700	Y	20	0	1.5
2014-10684	Ti834 Ring	700	Y	20	0	1.5
2014-10685	Ti834 Ring	700	Y	20	0	1.5
2014-10676	Ti834 Ring	1000	Y	20	0	1.5
2014-10677	Ti834 Ring	1000	Y	20	0	1.5
2014-10678	Ti834 Ring	1000	Y	20	0	1.5
2014-10679	Ti834 Ring	1000	Y	20	0	0.8
2014-10682	Ti834 Ring	1000	Y	20	0	0.8
2014-10683	Ti834 Ring	1000	Y	20	0	0.8

The elevated temperature LCF results for the Ti-834 forged material are displayed in table 18.

Table 18 Elevated temperature LCF results Ti-834 forged ring

STS NO.	Material	Exposure Time, @500(hrs)	Test Temp (°C)	R Ratio	Peak Strain (%)
2014-10694	Ti834 Ring	None	500	0	1.5
2014-10695	Ti834 Ring	None	500	0	1.5
2014-10696	Ti834 Ring	None	500	0	1.5
2014-10698	Ti834 Ring	None	500	0	0.9
2014-10699	Ti834 Ring	None	500	0	0.9
2015-12417	Ti834 Ring	100	500	0	1.5
2015-12419	Ti834 Ring	100	500	0	1.5
2015-12418	Ti834 Ring	100	500	0	0.9
2015-12420	Ti834 Ring	100	500	0	0.9

Creep results for the Ti-834 forged alloy are displayed in table 19. Time taken to 0.5% creep strain was reasonably consistent with 3 of the results.

Table 19 Creep results Ti-834 forged ring

STS NO.	Material	Exposure Time, @ 500 (hrs)	Test Temp (°C)	Stress (MPa)
2014-11066	Ti834 Ring	None	500	600
2014-11067	Ti834 Ring	None	500	600
2014-11068	Ti834 Ring	None	500	625
2014-11069	Ti834 Ring	None	500	625
*N6/3B/1B	Ti834 Ring	None	500	600
*N6/3B/1C	Ti834 Ring	None	500	600
*P6/3B/2B	Ti834 Ring	100	500	600
*P6/3B/2C	Ti834 Ring	100	500	600

*Tests performed at TIMET

The data recorded from FCP tests for Ti-834 forged alloy are shown in table 20.

Table 20 FCP results for Ti-834 forged ring

STS NO.	Material	Exposure Time, @450°C (hrs)	Test Temp (°C)	Stress (MPa)
2014-10703	Ti834 Ring	none	20	520

c. Centrifugally Cast Ti-834

The room temperature tensile results for the Ti-834 centrifugally cast alloy are shown in table 21. Reasonably high strength levels and good ductility levels were recorded for the unexposed material at room temperature. As with the forged alloy exposure times were modified to between 25 and 500 hours. The various exposure times were not found to have a significant effect on the strength of the material but significant reductions in tensile ductility were recorded in line with increasing exposure times when the oxide layer was retained. When this oxide layer was removed for testing some of the previously lost ductility was recovered for the longer exposure times.

Table 21 Room temperature tensile results centrifugally cast Ti-834

STS NO.	Material	Exposure @ 500°C (hrs)	Oxide Retained	Test Temp (°C)
2014-10901	Ti834 CC25mm	None	N/A	20
2014-10902	Ti834 CC25mm	None	N/A	20
2014-10903	Ti834 CC25mm	None	N/A	20
*MT6677(F14)	Ti834 CC13mm	None	N/A	20
*MT6678 (F15)	Ti834 CC22mm	None	N/A	20
*MT6678 (F20)	Ti834 CC25mm	None	N/A	20
*MT6673 (F9)	Ti834 CC13mm	None	N/A	20
*MT6674 (F9)	Ti834 CC13mm	None	N/A	20
*MT6675 (F11)	Ti834 CC25mm	None	N/A	20
*MT6676 (F11)	Ti834 CC25mm	None	N/A	20
2014-10907	Ti834 CC25mm	500	Y	20
2014-10908	Ti834 CC25mm	500	Y	20
2014-10909	Ti834 CC25mm	500	Y	20

2014-11561	Ti834 CC25mm	25	Y	20
2014-11558	Ti834 CC25mm	100	Y	20
2014-11560	Ti834 CC25mm	200	Y	20
*MT6732	Ti834 CC22mm	0	Y	20
*MT6733	Ti834 CC22mm	48	Y	20
*MT6734	Ti834 CC22mm	96	Y	20
*MT6735	Ti834 CC22mm	168	Y	20
*MT6686 (G14)	Ti834 CC13mm	100	Y	20
*MT6687 (G15)	Ti834 CC22mm	100	Y	20
*MT6688 (G20)	Ti834 CC25mm	100	Y	20
2014-11565	Ti834 CC25mm	25	N	20
2014-11567	Ti834 CC25mm	100	N	20
2014-11560	Ti834 CC25mm	200	N	20
2014-11570	Ti834 CC25mm	500	N	20

The room temperature tensile results for the Ti-834 centrifugally cast alloy which underwent further annealing cycles are shown in table 22. The 800^{o}C heat treatment was found to have little effect on the ductility of the alloy; however the previously lost ductility was recovered following the heat treatment at 1000^{o}C.

Table 22 Room temperature tensile results centrifugally cast Ti-834 annealed for further heat treatment

STS NO.	Material	Exposure @500^{o}C (hrs)	Anneal Temp (^{o}C)	Oxide Retained	Test Temp (^{o}C)
2014-11573	Ti834 CC25mm	500	800	N	20
2014-11572	Ti834 CC25mm	500	1000	N	20

Elevated temperature tensile results for the Ti-834 centrifugally cast alloy are shown in table 23.

Table 23 Elevated temperature tensile results centrifugally cast Ti-834

STS NO.	Material	Exposure @ 500°C (hrs)	Oxide Retained	Test Temp (°C)
2014-10904	Ti834 CC25mm	None	N/A	500
2014-10906	Ti834 CC25mm	None	N/A	500
2014-10915	Ti834 CC25mm	None	N/A	460
2014-10914	Ti834 CC25mm	None	N/A	480
2014-10910	Ti834 CC25mm	500	Y	500
2014-10911	Ti834 CC25mm	500	Y	500
2014-10912	Ti834 CC25mm	500	Y	500
*MT6695(H14)	Ti834 CC13mm	None	N/A	500
*MT6696(H15)	Ti834 CC22mm	None	N/A	500
*MT6697(H20)	Ti834 CC25mm	None	N/A	500

*Tests performed at TIMET

The tensile results for the HDH processed 13mm Ti-834 centrifugally cast material are shown in table 24.

Table 24 Tensile results hydrogenated Ti-834 Centrifugally cast 13mm

STS NO.	Material	Exposure @500°C (hrs)	Oxide Retained	Test Temp (°C)
2016-15169	Ti834 CC 13mm	None	N/A	20
2016-15170	Ti834 CC 13mm	None	N/A	20
2016-15171	Ti834 CC 13mm	None	N/A	20
2016-15172	Ti834 CC 13mm	None	N/A	500
2016-15302	Ti834 CC 13mm	None	N/A	500
2016-15303	Ti834 CC 13mm	None	N/A	500
2016-15301	Ti834 CC 13mm	100	Y	20
2016-15306	Ti834 CC 13mm	200	Y	20
2016-15297	Ti834 CC 13mm	500	Y	20

The tensile results for the HDH processed 23mm Ti-834 centrifugally cast material are shown in table 25.

Table 25 Tensile results hydrogenated Ti-834 Centrifugally cast 23mm

STS NO.	Material	Exposure @500°C (hrs)	Oxide Retained	Test Temp (°C)
2016-15290	Ti834 CC 23mm	None	N/A	20
2016-15291	Ti834 CC 23mm	None	N/A	20
2016-15292	Ti834 CC 23mm	None	N/A	20
2016-15293	Ti834 CC 23mm	None	N/A	500
2016-15294	Ti834 CC 23mm	None	N/A	500
2016-15295	Ti834 CC 23mm	None	N/A	500

The tensile results for the second batch of HDH processed Ti-834 centrifugally cast material are shown in table 26.

Table 26 Tensile results batch 2 hydrogenated Ti-834 Centrifugally cast material

STS NO.	Material	Exposure Time, @500°C (hrs)	Oxide Retained	Test Temp (°C)
2016-15726	Ti834 CC 13mm	none	N/A	20
2016-15727	Ti834 CC 13mm	none	N/A	20
2016-15729	Ti834 CC 23mm	none	N/A	20
2016-15731	Ti834 CC 23mm	none	N/A	20
2016-15732	Ti834 CC 23mm	none	N/A	20
2016-15733	Ti834 CC 23mm	none	N/A	500
2016-15734	Ti834 CC 23mm	none	N/A	500
2016-15735	Ti834 CC 23mm	none	N/A	500
2016-15720	Ti834 CC 23mm	100	N	20
2016-15721	Ti834 CC 23mm	100	N	20
2016-15723	Ti834 CC 23mm	100	N	20
2016-15722	Ti834 CC 23mm	100	N	500
2016-15724	Ti834 CC 23mm	100	N	500
2016-15725	Ti834 CC 23mm	100	N	500

Room temperature LCF results for the centrifugally cast Ti-834 alloy are illustrated in table 27.

Table 27 Room temperature LCF results centrifugally cast Ti-834

STS NO.	Material	Exposure Time, @500(hrs)	Test Temp (°C)	R Ratio	Peak Strain (%)
2014-11052	Ti834 CC25mm	None	20	0	1.0
2014-11053	Ti834 CC25mm	None	20	0	1.0
2014-11054	Ti834 CC25mm	None	20	0	1.0
2014-11055	Ti834 CC25mm	None	20	0	0.55
2014-11056	Ti834 CC25mm	None	20	0	0.55
2014-11057	Ti834 CC25mm	None	20	0	0.55
2014-11048	Ti834 CC25mm	500	20	0	0.55
2014-11049	Ti834 CC25mm	500	20	0	1.0

A limited amount of elevated temperature testing fatigue testing was performed on centrifugally cast Ti-834, giving results shown in Table 28.

Table 28 Elevated temperature LCF results centrifugally cast Ti-834

STS NO.	Material	Exposure Time, @500(hrs)	Test Temp (°C)	R Ratio	Peak Strain (%)
2014-11058	Ti834 CC25mm	500	500	0	0.65
2014-11059	Ti834 CC25mm	500	500	0	0.65

Creep results for the Ti-834 centrifugally cast alloy are shown in table 29.

Table 29 Creep results centrifugally cast Ti-834

STS NO.	Material	Exposure Time, @500 (hrs)	Test Temp (°C)	Stress (MPa)
2014-11070	Ti834 CC25mm	None	500	450
2014-11071	Ti834 CC25mm	None	500	500
2014-11072	Ti834 CC25mm	None	500	550

The data recorded from FCP tests for Ti-834 centrifugally cast alloy are shown in table 30.

Table 30 FCP results centrifugally cast Ti-834

STS NO.	Material	Exposure Time, @450°C (hrs)	Test Temp (°C)	Stress (MPa)
2014-10965	Ti-834 CC 25mm	none	20	520

d. Gravity Cast Ti-834

The room temperature tensile results for the 25mm section Ti-834 gravity cast alloy are shown in table 31, together with results after 500 hour exposure time.

Table 31 Tensile results gravity cast Ti-834 25mm

STS NO.	Material	Exposure Time, @ 500°C (hrs)	Oxide Retained	Test Temp (°C)
2014-11292	Ti834 GC	None	N/A	20
2014-11293	Ti834 GC	None	N/A	20
2014-11296	Ti834 GC	None	N/A	20
2014-11289	Ti834 GC	500	Y	20
2014-11290	Ti834 GC	500	Y	20
2014-11291	Ti834 GC	500	Y	20
*2015-12840	Ti834 GC	None	N/A	20
*2015-12838	Ti834 GC	100	Y	20
*2015-12842	Ti834 GC	None	N/A	20
*2015-12841	Ti834 GC	100	Y	20

*Heat treatment trial-1120°C/965°C/621°C

Room temperature LCF results for the gravity cast Ti-834 alloy are illustrated in table 32, at strain levels of 0.55% and 1.0%. Further tests were carried out after an exposure time of 500 hours.

Table 32 Room temperature LCF results gravity cast Ti-834 25mm

STS NO.	Material	Exposure Time, @500(hrs)	Test Temp (°C)	R Ratio	Peak Strain (%)
2014-11171	Ti834 GC25mm	None	20	0	0.55
2014-11172	Ti834 GC25mm	None	20	0	0.55
2014-11173	Ti834 GC25mm	None	20	0	0.55
2014-11174	Ti834 GC25mm	None	20	0	1.0
2014-11175	Ti834 GC25mm	None	20	0	1.0
2014-11176	Ti834 GC25mm	None	20	0	1.0
2014-11167	Ti834 GC25mm	500	20	0	1.0
2014-11168	Ti834 GC25mm	500	20	0	0.55

Room temperature LCF results for the gravity cast Ti-834 alloy are illustrated in table 33.

Table 33 Elevated temperature LCF results gravity cast Ti-834 25mm

STS NO.	Material	Exposure Time, @500(hrs)	Test Temp (°C)	R Ratio	Peak Strain (%)
2014-11177	Ti834 GC25mm	None	500	0	0.65
2014-11178	Ti834 GC25mm	None	500	0	0.65

Creep results for the Ti-834 gravity cast alloy are shown in table 34. Significant strain values were seen on loading at a stress of 550MPa.

Table 34 Creep results gravity cast Ti-834

STS NO.	Material	Exposure Time, @500 (hrs)	Test Temp (°C)	Stress (MPa)
2014-11772	Ti834 Gravity cast	None	500	550

The data recorded from FCP tests for Ti-834 gravity cast alloy are shown in table 35.

Table 35 FCP results gravity cast Ti-834

STS NO.	Material	Exposure Time, @450°C (hrs)	Test Temp (°C)	Stress (MPa)
2014-11157	Ti-834 GC 25mm	None	20	520

e. Ti-834 Sheet

Tensile results at room and elevated for the Ti-834 2mm sheet are displayed in table 36, together with tests after elevated temperature exposure.

Table 36 Tensile results Ti-834 2mm sheet

STS NO.	Material	Exposure Time, @500°C (hrs)	Oxide Retained	Test Temp (°C)
2015-12517	Ti-834 2mm sheet	None	N/A	20
2015-12518	Ti-834 2mm sheet	None	N/A	20
2015-12837	Ti-834 2mm sheet	None	N/A	500
2015-13229	Ti-834 2mm sheet	None	N/A	500
2015-12520	Ti-834 2mm sheet	100	Y	20
2015-13230	Ti-834 2mm sheet	100	Y	20
2015-13231	Ti-834 2mm sheet	100	Y	500
2015-13233	Ti-834 2mm sheet	100	Y	500

Room temperature LCF results for the Ti-834 2mm sheet are displayed in table 37.

Table 37 Room temperature LCF results Ti-834 2mm sheet

STS NO.	Material	Exposure Time, @500(hrs)	Test Temp (°C)	R Ratio	Peak Stress (MPa)
2015-12834	Ti-834 2mm sheet	None	20	0.01	750
2015-13237	Ti-834 2mm sheet	None	20	0.01	750
2015-12833	Ti-834 2mm sheet	None	20	0.01	950
2015-13236	Ti-834 2mm sheet	None	20	0.01	950

Elevated temperature LCF results for the Ti-834 2mm sheet are shown in table 38.

Table 38 Elevated temperature LCF results Ti-834 2mm sheet

STS NO.	Material	Exposure Time, @500(hrs)	Test Temp (°C)	R Ratio	Peak Stress (MPa)
2015-13262	Ti-834 2mm sheet	None	500	0.01	750
2015-12835	Ti-834 2mm sheet	None	500	0.01	750
2015-12836	Ti-834 2mm sheet	None	500	0.01	650
2015-13264	Ti-834 2mm sheet	None	500	0.01	650

Room temperature and elevated temperature tensile results for the Ti-834 4mm sheet, before and after elevated temperature exposure, are displayed in table 39.

Table 39 Tensile results Ti-834 4mm sheet

STS NO.	Material	Exposure Time, @500°C (hrs)	Oxide Retained	Test Temp (°C)
2015-13223	Ti-834 4mm sheet	None	N/A	20
2015-13224	Ti-834 4mm sheet	None	N/A	20
2015-13225	Ti-834 4mm sheet	None	N/A	500
2015-13226	Ti-834 4mm sheet	None	N/A	500
2015-13221	Ti-834 4mm sheet	100	Y	20
2015-13222	Ti-834 4mm sheet	100	Y	20
2015-13227	Ti-834 4mm sheet	100	Y	500
2015-13228	Ti-834 4mm sheet	100	Y	500

The room temperature LCF results for the Ti-834 4mm sheet are displayed in table 40.

Table 40 LCF results Ti-834 4mm sheet

STS NO.	Material	Exposure Time, @500(hrs)	Test Temp (°C)	R Ratio	Peak Stress (MPa)
2015-13235	Ti-834 4mm sheet	None	20	0.01	950
2015-13234	Ti-834 4mm sheet	None	20	0.01	750

Room and elevated temperature tensile results for the Ti-834 2mm welded sheet are displayed in table 41, together with further tests after exposure at 500°C for 100 hours.

Table 41 Tensile results Ti-834 2mm welded sheet

STS NO.	Material	Exposure Time, @500°C (hrs)	Oxide Retained	Test Temp (°C)
2015-14382	Ti-834 2mm weld sheet	None	N/A	20
2015-14388	Ti-834 2mm weld sheet	None	N/A	20
2015-14386	Ti-834 2mm weld sheet	None	N/A	500
2015-14387	Ti-834 2mm weld sheet	None	N/A	500
2015-14379	Ti-834 2mm weld sheet	100	Y	20
2015-14381	Ti-834 2mm weld sheet	100	Y	20
2015-14376	Ti-834 2mm weld sheet	100	Y	500
2015-14377	Ti-834 2mm weld sheet	100	Y	500

Room temperature LCF results for the Ti-834 2mm welded sheet are displayed in table 42.

Table 42 Room temperature LCF results Ti-834 2mm welded sheet

STS NO.	Material	Exposure Time, @500(hrs)	Test Temp (°C)	R Ratio	Peak Stress (MPa)
2015-14378	Ti-834 2mm weld sheet	None	20	0.01	950
2015-14381	Ti-834 2mm weld sheet	None	20	0.01	950
2015-14390	Ti-834 2mm weld sheet	None	20	0.01	750
2015-14391	Ti-834 2mm weld sheet	None	20	0.01	750

Elevated temperature LCF results for the Ti-834 2mm welded sheet are displayed in table 43.

Table 43 Elevated temperature LCF results Ti-834 2mm welded sheet

STS NO.	Material	Exposure Time, @500(hrs)	Test Temp (°C)	R Ratio	Peak Stress (MPa)
2015-14384	Ti-834 2mm weld sheet	None	500	0.01	650

Room and elevated temperature tensile results for the Ti-834 4mm welded sheet are displayed in table 44, together with further tests after exposure at 500°C for 100 hours.

Table 44 Tensile results Ti-834 4mm welded sheet

STS NO.	Material	Exposure Time, @500°C (hrs)	Oxide Retained	Test Temp (°C)
2015-14525	Ti-834 4mm weld sheet	None	N/A	20
2015-14526	Ti-834 4mm weld sheet	None	N/A	20
2015-14527	Ti-834 4mm weld sheet	None	N/A	500
2015-14528	Ti-834 4mm weld sheet	None	N/A	500
2015-14529	Ti-834 4mm weld sheet	100	Y	20
2015-14530	Ti-834 4mm weld sheet	100	Y	20
2015-14531	Ti-834 4mm weld sheet	100	Y	500
2015-14532	Ti-834 4mm weld sheet	100	Y	500

Room temperature LCF results for the Ti-834 4mm welded sheet are displayed in table 45.

Table 45 Room temperature LCF results Ti-834 4mm welded sheet

STS NO.	Material	Exposure Time, @500(hrs)	Test Temp (°C)	R Ratio	Peak Stress (MPa)
2015-14533	Ti-834 4mm weld sheet	None	20	0.01	950
2015-14534	Ti-834 4mm weld sheet	None	20	0.01	750
2015-14535	Ti-834 4mm weld sheet	None	20	0.01	950
2015-14536	Ti-834 4mm weld sheet	None	20	0.01	750

Elevated temperature LCF results for the Ti-834 4mm welded sheet are displayed in table 46.

Table 46 Elevated temperature LCF results Ti-834 4mm welded sheet

STS NO.	Material	Exposure Time, @500(hrs)	Test Temp (°C)	R Ratio	Peak Stress (MPa)
2015-14537	Ti-834 4mm weld sheet	None	500	0.01	750
2015-14538	Ti-834 4mm weld sheet	None	500	0.01	650

4. Discussion

4.1 Tensile Results

Initial tensile testing of Ti-6242S centrifugally cast material found that the material had reasonably high strength and ductility in both 13mm and 25mm sections. This was evident at both room and elevated temperatures. Exposure at the current operating temperature of Ti-6242S (450°C) for 1000 hours was not found to have a dramatic effect on properties; only slightly reducing the ductility of the material when it was tested with the resultant oxide layer retained.

After positive results from the initial room and elevated temperature tensile testing of Ti-834 centrifugally cast material, it soon became apparent that there was a considerable loss of ductility in the alloy after prolonged exposure at the proposed operating temperature of 500°C. This loss of

ductility became the main focus of the project and as a result further tests were performed on the alloy after different exposure times. It can clearly be seen in figure 19 that a reduction in ductility is seen in line with increasing exposure times when the resultant oxide layer is retained at the surface.

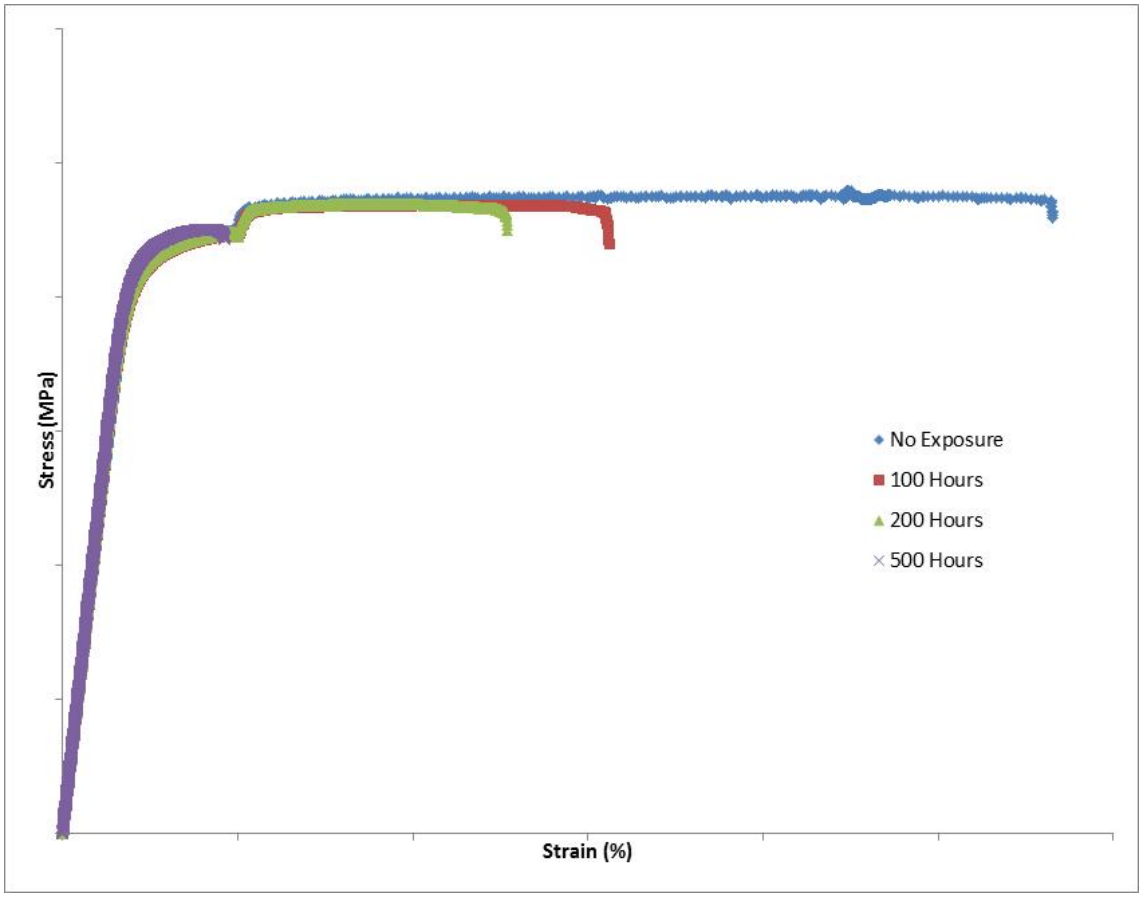

Figure 19 Room temperature tensile curves for Ti-834 centrifugally cast alloy after various exposure times, oxide retained

In order to determine if this oxide layer or changes caused to the bulk of the alloy were responsible for the loss in ductility, it was decided to perform tests on exposed specimens which then had the oxide layer removed before testing. By removing the oxide layer it is clear to see in figure 20 that a significant proportion of this lost ductility is recovered. Removing the oxide layer resulted in similar ductility values for the three different exposure times, but there was still a significant reduction in ductility when compared to the material in the unexposed condition. These results show that changes in the bulk of the material after exposure are responsible for the remaining loss in ductility.

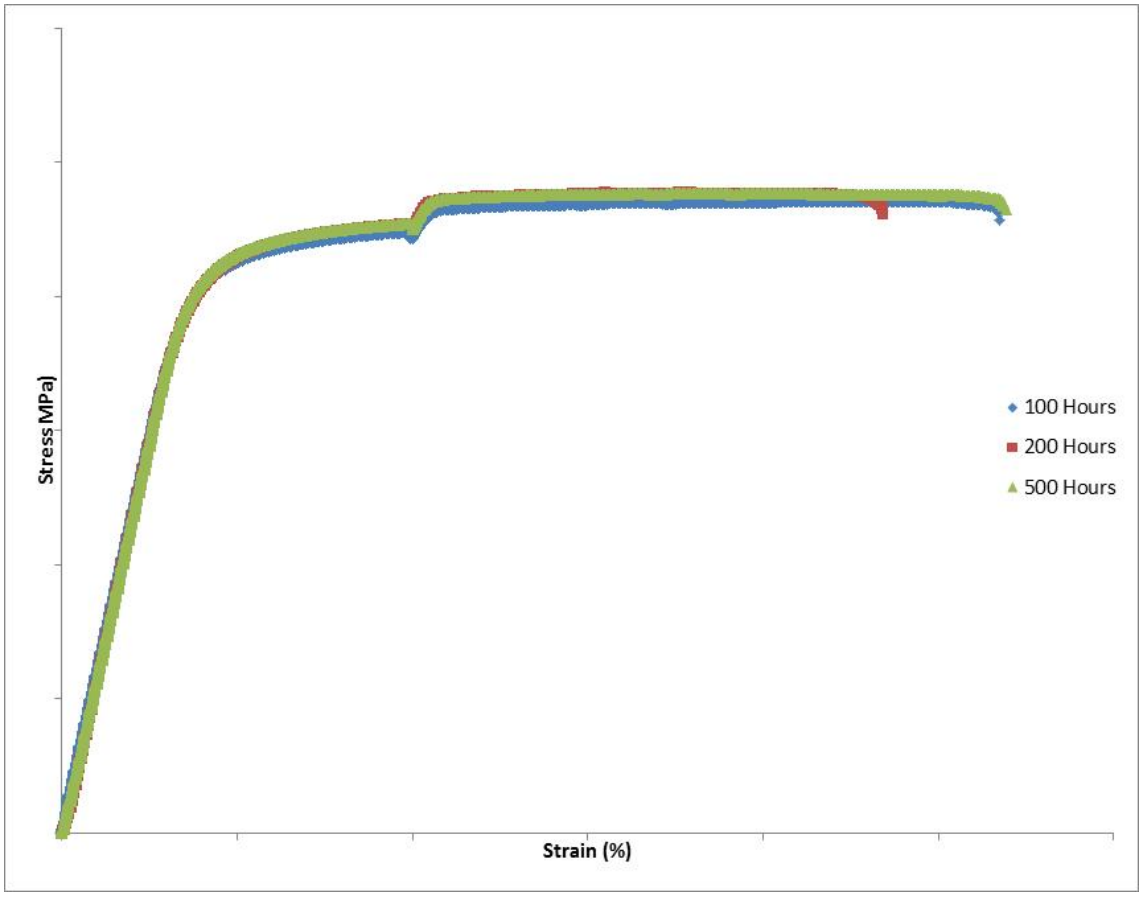

Figure 20 Room temperature tensile curves for Ti-834 centrifugally cast alloy after various exposure times, oxide removed

As previously mentioned α_2 and silicide precipitation are thought to detrimental to ductility when present in large enough volumes. In order to determine the effect α_2 precipitation has on the ductility of centrifugally cast Ti-834, previously exposed (500h at 500°C) tensile specimens were subjected to another heat treatment. Calculations performed using the JMatPro programme (figure 21) suggested the solvus temperature of the α_2 precipitates to be 675°C. However this contradicted slightly with information in previous literature [9] that claimed the α_2 precipitate solvus temperature in Ti-834 was 750°C. It was decided to apply an annealing cycle of 2 hours at 800°C to dissolve the α_2 precipitates.

Figures 22 a and b illustrate α_2 precipitates in the cast material exposed for 500h at 500°C, and the cast material previously exposed under the same conditions plus the further heat treatment at 800°C respectively. After the initial exposure the α phase is densely populated by α_2 precipitates of approximately 10-60nm in diameter. The image in Fig. 22b shows that the majority of the α_2 precipitates were dissolved by the 800°C heat treatment, though there are still some precipitates up to 40nm in diameter present. The α_2 precipitates visible after the 800°C heat treatment are likely to

have precipitated out on cooling from the annealing temperature. It is reasonable to expect that all of the pre-existing α_2 precipitates were dissolved during this heat cycle where the temperature was approximately 50°C above the α_2 solvus temperature of 750°C.

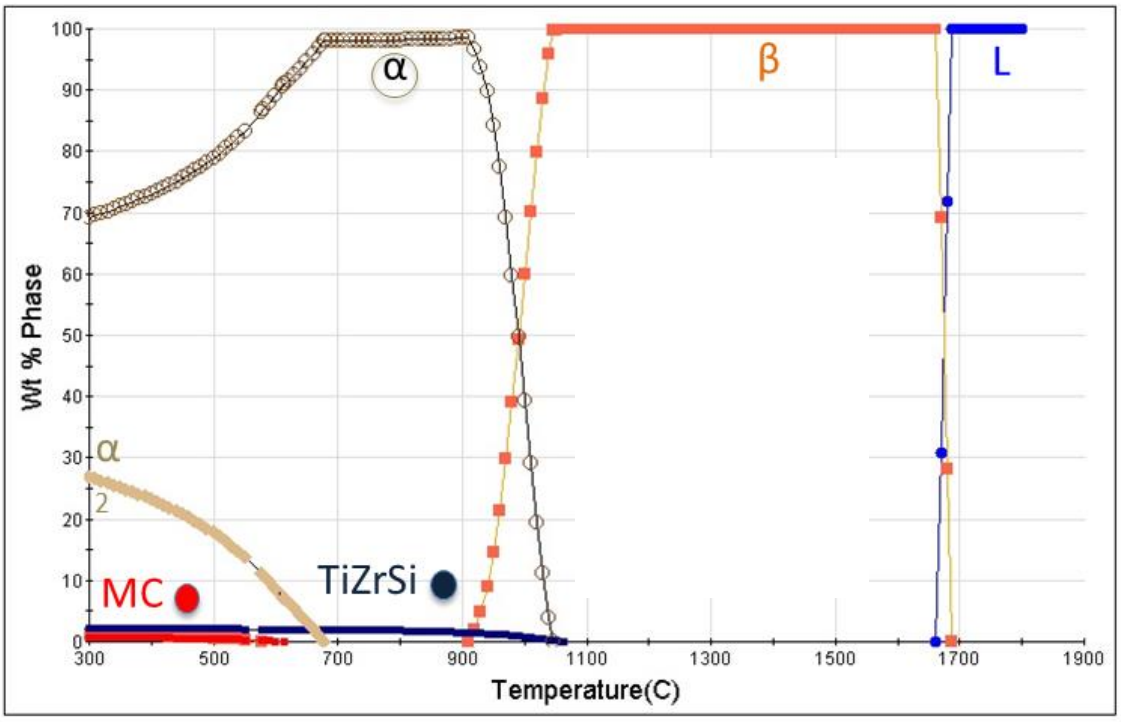

Figure 21 Calculations performed using JMatPro programme

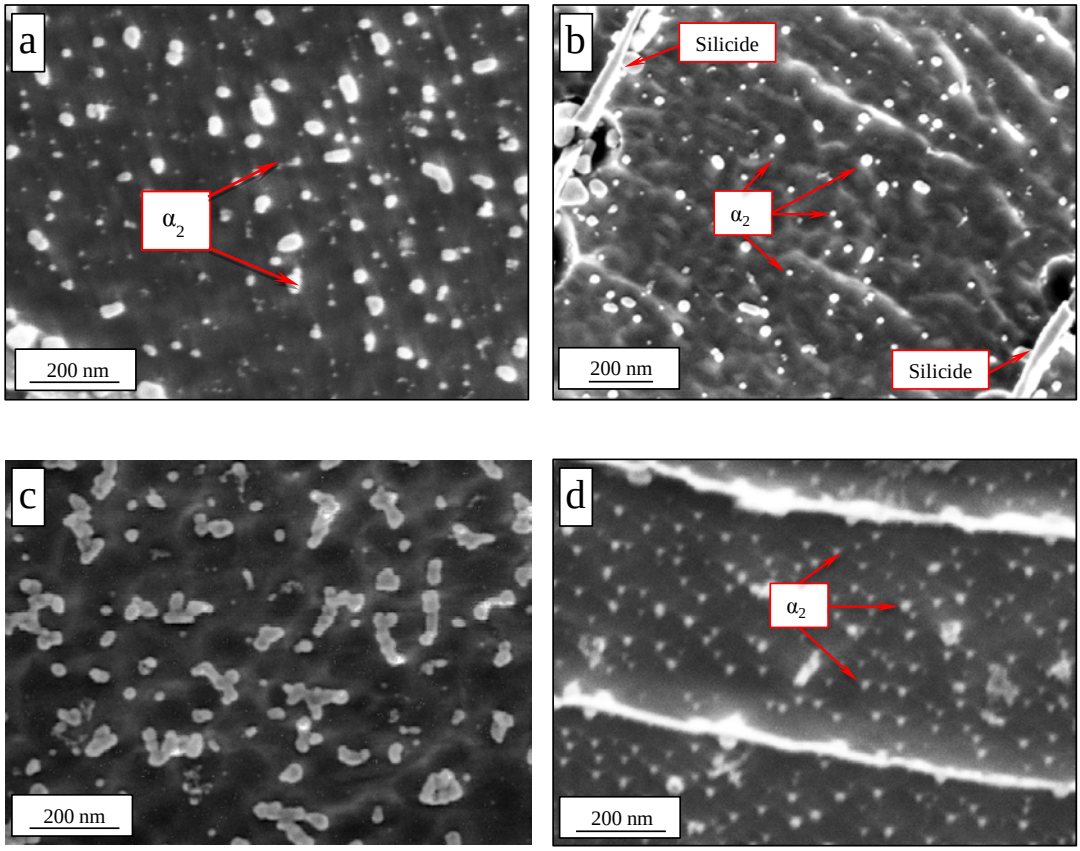

Figure 22 Illustration of α_2 precipitates found in cast alloy, a) after exposure at 500°C for 500 hours, b) after exposure at 500°C for 500 hours plus 2 hours at 800°C, c) after exposure at 500°C for 500 hours plus 2 hours at 1000°C, d) forged alloy after exposure at 500°C for 500 hours

The tensile curves shown in figure 23 indicate that α_2 precipitation has little effect on the ductility of the centrifugally cast Ti-834 material after exposure.

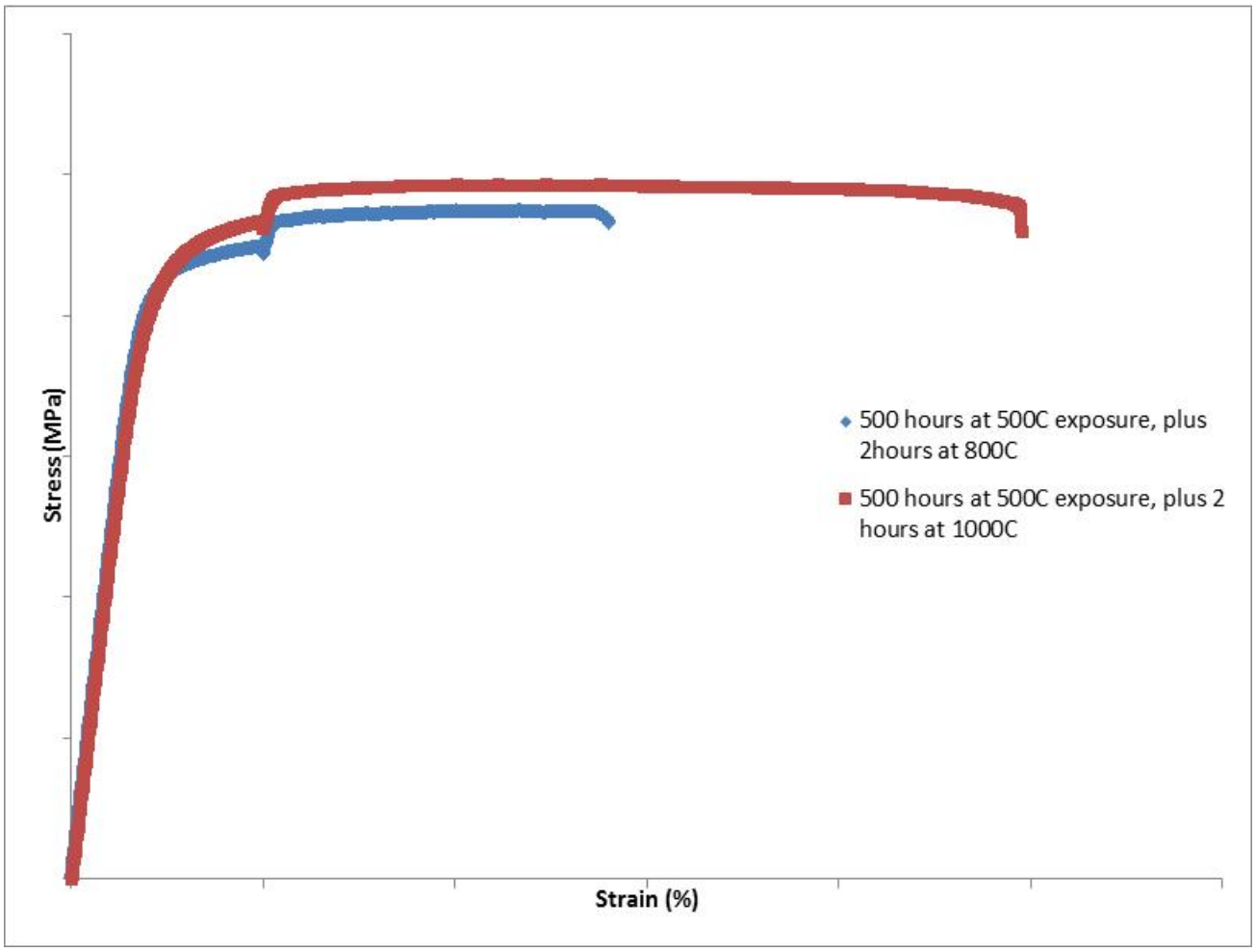

Figure 23 Room temperature tensile curves for previously exposed (500h @500°C) Ti-834 centrifugally cast alloy after extra heat treatments, oxide removed

In order to determine the effect silicide precipitation has on the ductility of centrifugally cast Ti-834, again previously exposed (500h at 500°C) tensile specimens were subjected to a heat treatment at 1000°C for 2 hours to dissolve any silicides present. This temperature was again selected using a combination of JMatPro programme (figure 21) which determined the solvus temperature to be 1050°C, and literature [6] which suggested a solvus temperature of 990°C. It was decided to use a temperature of 1000°C as this would be above the silicide solvus temperature [6] and below the beta transus (β_T) of the material which was approximately 1025°C.

Figure 23 illustrates that the majority of the lost ductility was recovered when specimens were heat treated at 1000°C/2h to dissolve silicides. These results indicate that the presence of silicides has a vital contribution in the ductility regression in the centrifugally cast Ti-834 alloy. Figure 22c illustrates the alloy after the 1000°C heat treatment; this shows that the alloy contains not only a higher concentration of α_2 precipitates than those found in the originally exposed material, but that they are generally coarser with diameters of up to 100nm. This also suggests that although the α_2 re-

precipitated during cooling and formed more and larger α_2 precipitates they did not affect the tensile ductility of the material.

Figure 24a and 20d show high-resolution backscatter SEM images for centrifugally cast Ti-834 prior and after 500°C/500h exposure, respectively. The 2D EDX silicon and zirconium maps for Figure 24a are shown in and 24b and 24c and for Figure 24d in 24e and 24f, respectively. As shown in Figure 24a, small silicides (~ 400-900 nm in diameter) with irregular shape are located on the α/β phase boundaries throughout the cast material prior to any exposure. Figure 24d-f, show the 500°C/500h exposure increased the concentration of silicides greatly in the centrifugally cast alloy. The silicides were also found to be much coarser than those seen in the unexposed material; up to 2.5µm in diameter. Furthermore, the exposure at 500°C for 500h caused the existing silicides to coarsen on α/β phase boundaries and a large number of silicides precipitates were observed within the α lamellae. It is evident from Figure 24g, that the silicide coarsening on α/β phase boundaries caused large voids formation around the precipitates. This is an indication that the silicide lost its coherency with the α matrix at this stage.

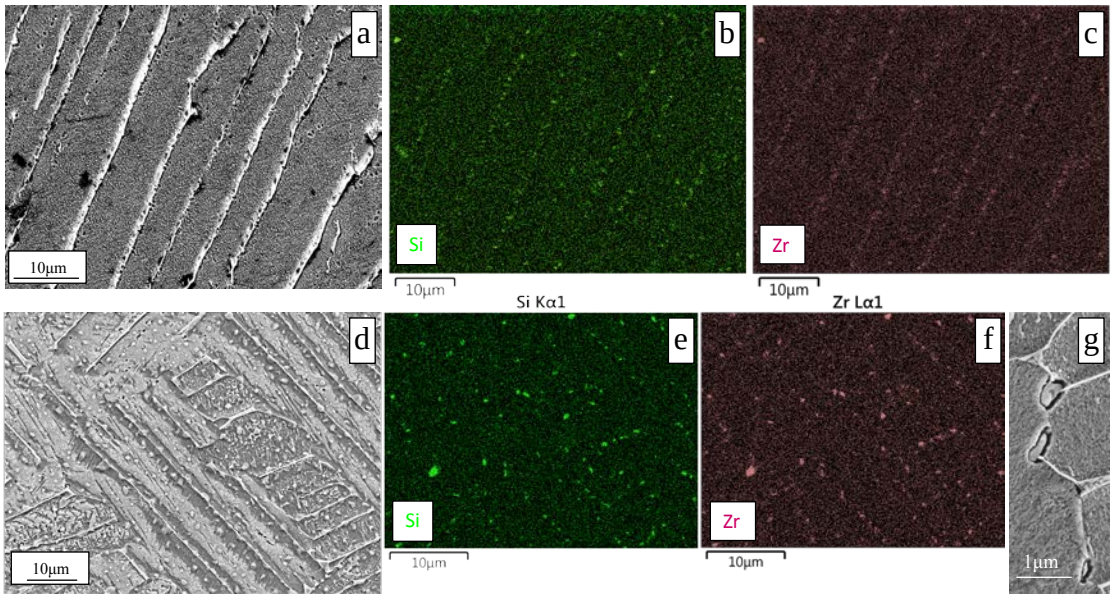

Figure 24 high-resolution backscatter SEM images for centrifugally cast Ti-834, a) prior to 500°C/500h exposure, b) 2D EDX silicon map for Figure 24a, c) 2D EDX zirconium map for Figure 24a, d) after 500°C/500h exposure, e) 2D EDX silicon map for Figure 24d, f) 2D EDX zirconium map for Figure 24d, g) large void formation around the precipitates silicide caused by coarsening on α/β phase boundaries.

Figure 25 a-c shows the microstructure (a) and EDX chemical analyses (b and c) of centrifugally cast Ti-834 alloy following 500ºC/500h exposure and heat treatment at 800ºC/2h. It is clear from the figure that 800°C/2h heat treatment has enabled further silicide precipitation and the coarsening of existing silicides to occur. As shown in Figure 25d, further voids were formed on silicide/matrix

boundaries after 800°C/2h annealing. It appears that further silicide precipitation, coarsening and disbonding during 800°C/2h annealing have greater effect on the ductility and overcome most of the recovery that might have occurred from dissolving the α_2 precipitates. Figure 25e-g shows the microstructure and chemical analyses of centrifugally cast Ti-834 alloy following 500°C/500h exposure and 1000°C/2h heat treatment. As shown in the figures the vast majority of the microstructure was free from silicides. Further analysis of the microstructure; see Figure 25e-h, showed that there were however isolated regions that still contained some silicides after the 1000°C/2h heat treatment. This may be correlated to the alloying element heterogeneous distribution, where some areas have nominally higher silicon content than other areas. This occurs due to the high partitioning coefficient silicon has in titanium, which allows it to partition to the last areas to freeze on cooling. Furthermore, the silicide solvus temperature calculated using JMATPro was 1050°C, see Figure 21, 50° C above the heat treatment temperature used here. Therefore, a small volume fraction of silicide may be expected after 1000°C/2h annealing. The heat treatment also caused α laths to coarsen with laths up to 11µm in width. This coarsening might have a negative effect on ductility as effective slip lengths would become longer post 1000°C heat treatment.

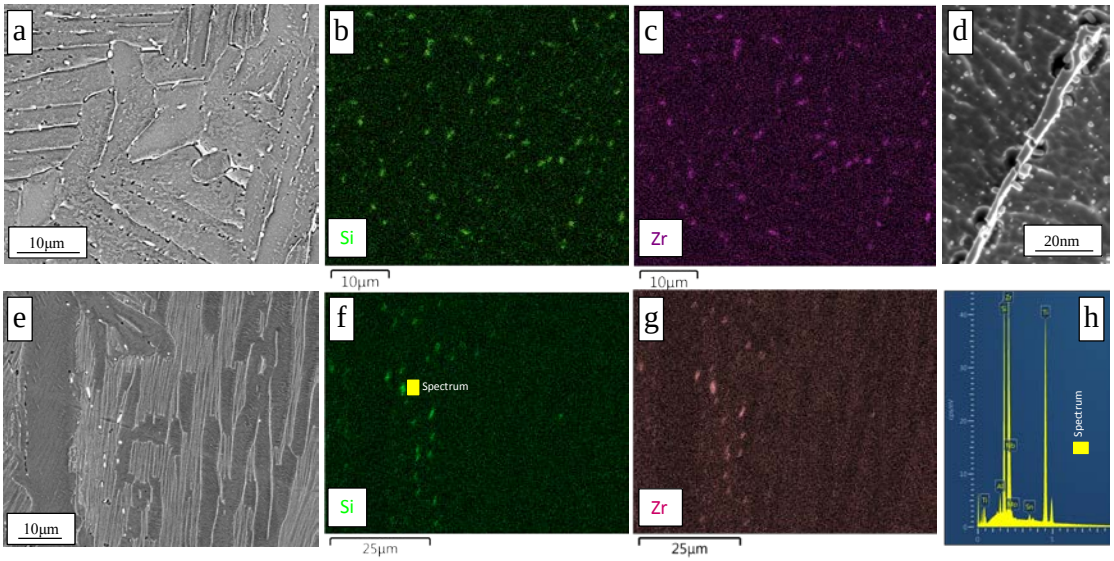

Figure 25 high-resolution backscatter SEM images for centrifugally cast Ti-834 previously exposed 500h/500°C, a) subjected to 800°C/2h exposure, b) 2D EDX silicon map for Figure 25a, c) 2D EDX zirconium map for Figure 25a, d) further void formation, e) subjected to 800°C/2h exposure, f) 2D EDX silicon map for Figure 25e, c) 2D EDX zirconium map for Figure 25e,h) EDX spectrum from figure 25f.

An attempt was made to improve the tensile ductility of the centrifugally cast Ti-834 by refining the microstructure, this was attempted by putting the material through a hydrogenation and

dehydrogenation (HDH) process. The microstructures of the 13mm and 23mm products shown in in figures 11and 12 shows that this was achieved with both products displaying finer prior β grains; especially so with the 13mm material. The internal structure of the grains was also modified by this process which developed more of a Widmanstatten structure, not the coarse α laths seen in the standard material. The potential of this process can be seen by 2 tensile results from the 13mm material where an elongation of 10.3% was seen at 500°C and another where 13% elongation is recorded at room temperature after a 100 hour exposure. However the possible Improvement in ductility was undermined by the dehydrogenation process where it proved very difficult to remove sufficient hydrogen from the material, causing embrittlement of the material leading to the poor ductility seen for the majority of the tests. Hydrogen analysis performed on the material found approximately 110ppm hydrogen remaining in the material tested.

The amount of hydrogen retained after the dehydrogenation process also compromised the testing of specimens after different exposure times. All but three of the specimens that were exposed at 500°C were found to have cracks present on the gauge of the test specimen as seen figure 26.

The results attained for the second batch of hydrogenated material further show the potential of the process with improved ductility and more consistency in the results when compared to the initial hydrogenated material.

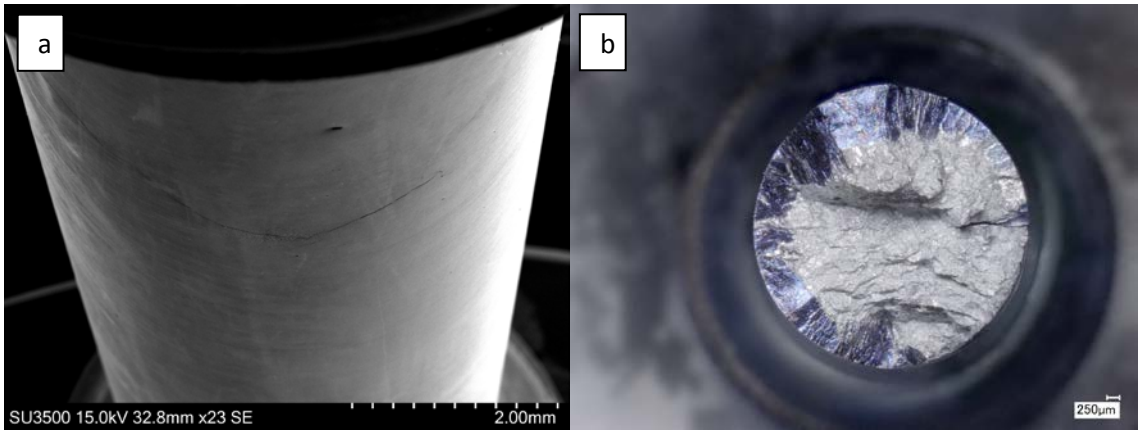

Figure 26 a) Crack found on gauge of hydrogenated Ti-834 centrifugally cast specimen exposed for 200h/550°C, b) fracture surface of hydrogenated Ti-834 centrifugally cast specimen exposed for 200h/550°C tensile specimen illustrating oxidation where material had cracked during exposure

As shown in Figure 27, the forged material in the unexposed and exposed for 100, 200 and 500 hour conditions is stronger and more ductile than its centrifugally cast equivalent. This can be seen in tables 15 and 21 which show that the forged material in the unexposed condition has a significantly higher tensile strength with both the UTS and 0.2% proof stress values being approximately 10% higher than those recorded for the centrifugally cast material. Ductility was also far greater in the

forged material where the elongation was ~%60 greater than achieved by the cast material. Unlike the Ti-834 centrifugally cast material no loss of ductility was recorded in line with increasing exposure times for the forged alloy.

As illustrated in figure 23d the forged material which retained its ductility after 500°C/500h exposure was found to have a high concentration of α_2 precipitates, however these were much finer than those found in the centrifugally cast Ti-834 alloy; with typical diameters of 10-20nm. It appeared that the homogenous distribution of the very fine α_2 precipitates and their high coherency with the α phase matrix may have assisted in alloy strengthening of the Ti-834 forged alloy with good ductility, especially at high temperatures. The silicides found in the forged material had a similar irregular shape to those found in the centrifugally cast alloy; however as with the α_2 precipitates they were much smaller in size; in the range of 80nm – 200nm. The fine silicide size in the wrought alloy is attributed to the smaller volume fraction of β phase in between α lamellaes in the bimodal microstructure of the forged material. It appears there is no significant increase in the overall concentration of silicides present in the bimodal microstructure. This further explains the ductility preservation of the forged Ti-834 alloy after 500°C/500h exposure. It was also rather apparent that existing silicides did not coarsened during the exposure; their diameters remained stable at approximately 100-200 nm.

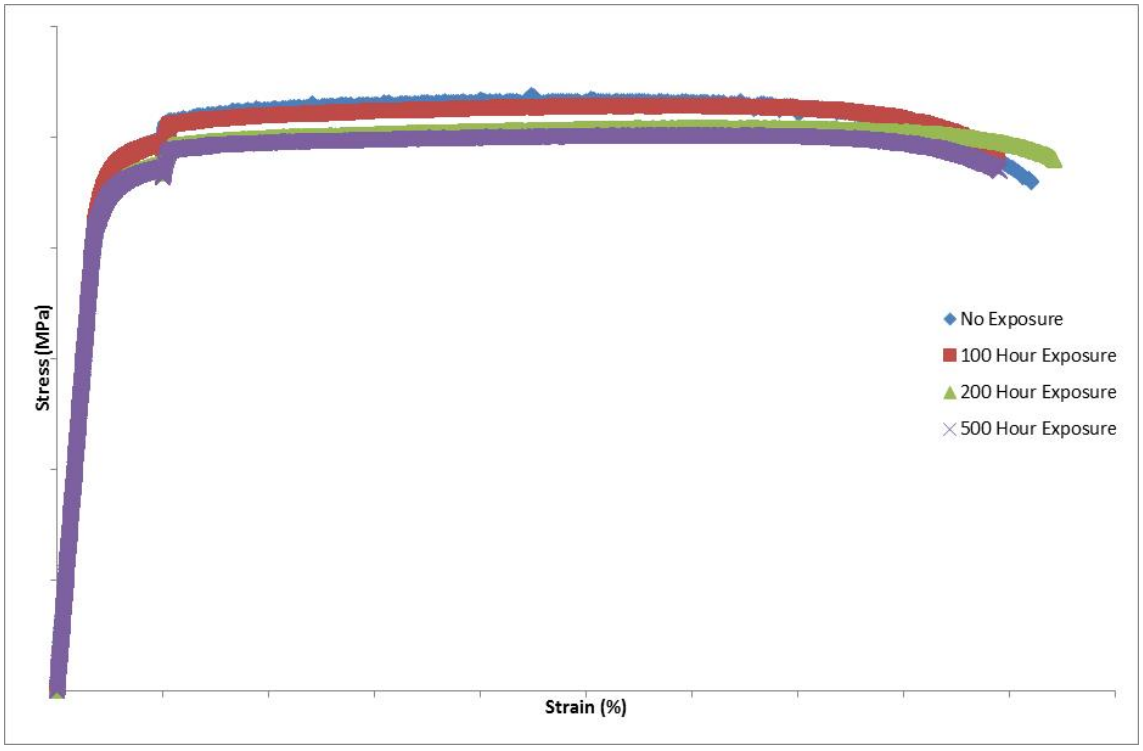

Figure 27 Room temperature tensile curves for Ti-834 forged material after various exposure times

Although the Ti-834 gravity cast material delivered reasonable strength levels for the unexposed material at room temperature, the ductility levels were significantly lower when compared to the centrifugally cast material . Testing the material with the oxide layer retained after elevated temperature exposure reduced the ductility of the material to virtually zero as seen in figure 28. After modified processing temperatures failed to improve the properties of the material significantly it was decided to halt further testing and concentrate on the centrifugally cast material.

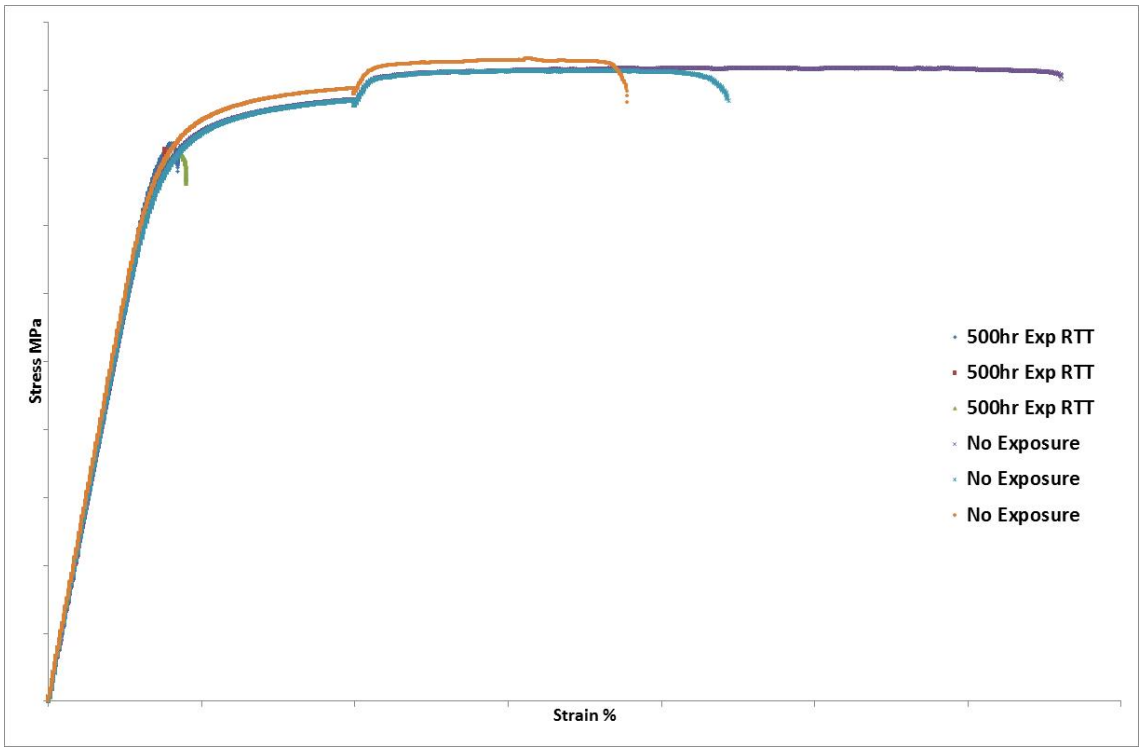

Figure 28 Room temperature tensile curves for Ti-834 gravity cast material

The tensile performance of Ti-834 welded 2mm sheet generally compared well to the base 2mm sheet material in both the exposed and unexposed conditions. Both strength and ductility were retained in the welded sheet when final fractures occurred away from the heat affected zone (HAZ) of the specimen. Where failures occurred at the HAZ then ductility was significantly reduced. The tensile performance of the Ti-834 4mm welded sheet was also comparable to the base material, again both strength and elongation were retained in the exposed and unexposed conditions at room and elevated temperatures.

a. LCF

All strain levels used during the project were suggested by GKN at the outset. Room temperature tests, on cast products were to be carried out at 0.55 and 1% peak strain levels. At elevated temperature, tests on cast products were to be carried out at 0.65 and 1.2% peak strain levels. For the forged material higher strain levels were applied; at room temperature strain levels of 0.8 and 1.5% were applied, while at room temperature the lower level was increased to 0.9%. It was initially intended that all LCF tests on sheet products were to be performed under strain control conditions. However this was not possible due to buckling of the specimens after initial yielding. It was decided that all sheet and welded sheet would be tested under stress control conditions. At room temperature stress levels of 750 and 950MPa were applied, while at elevated temperature these were reduced to 650 and 750MPa.

A pattern of results emerged early in the LCF testing where at lower strain or stress levels long lives were achieved. When the higher strain or stress level was applied lives were much shorter. Figure 29 illustrates the fatigue life of the Ti-6242S 13mm cast product. This trend was repeated for the 25mm Ti-6242S cast product shown in figure 30.

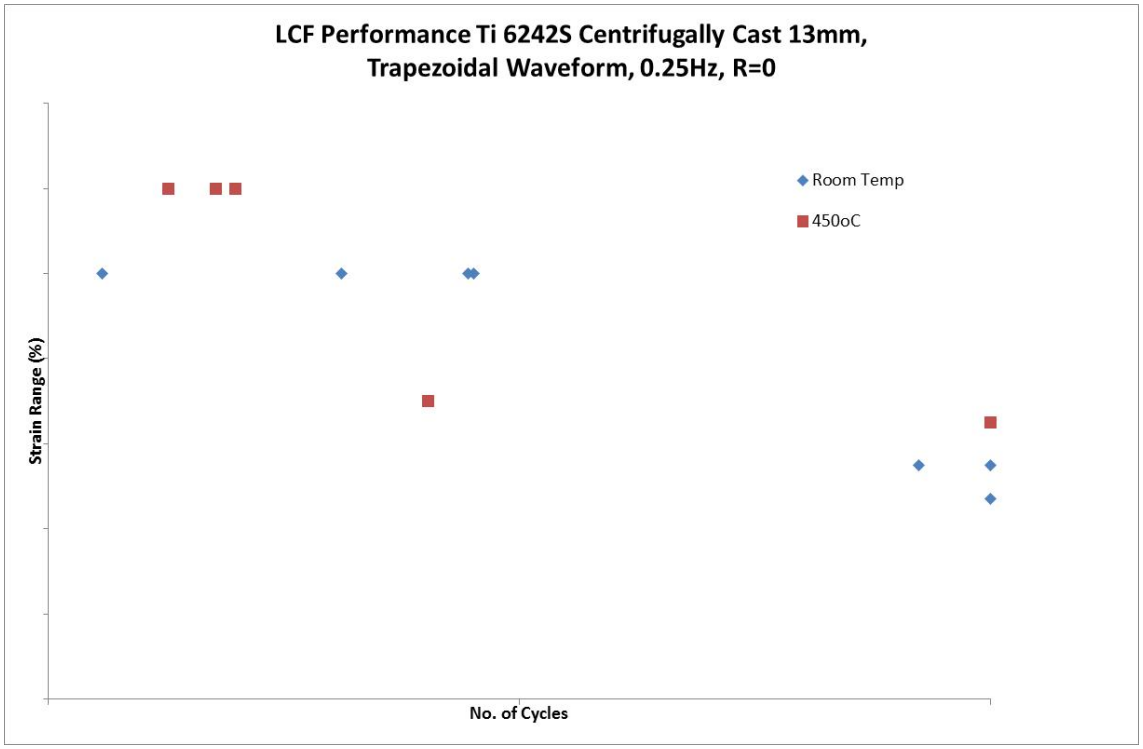

Figure 29 Peak strain versus cycles to failure for Ti-6242S 13mm product

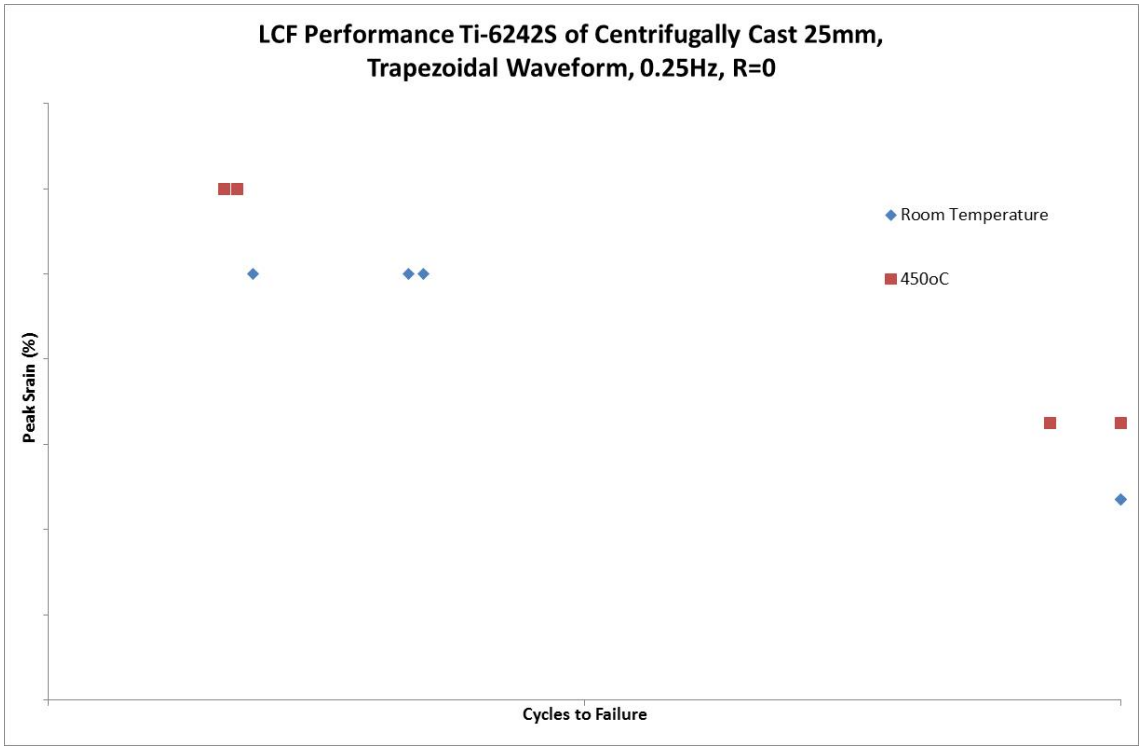

Figure 30 Peak strain versus cycles to failure for Ti-6242S 25mm product

At room temperature the Ti-6242S 2mm (figure 31) and 4mm (figure 32) sheet material produced similar results to the cast products. However while the elevated temperature high stress lives were similar the low stress lives were far shorter than those seen with the cast products. Analysis of the fracture surfaces (figure 33) showed no reason for these premature failures.

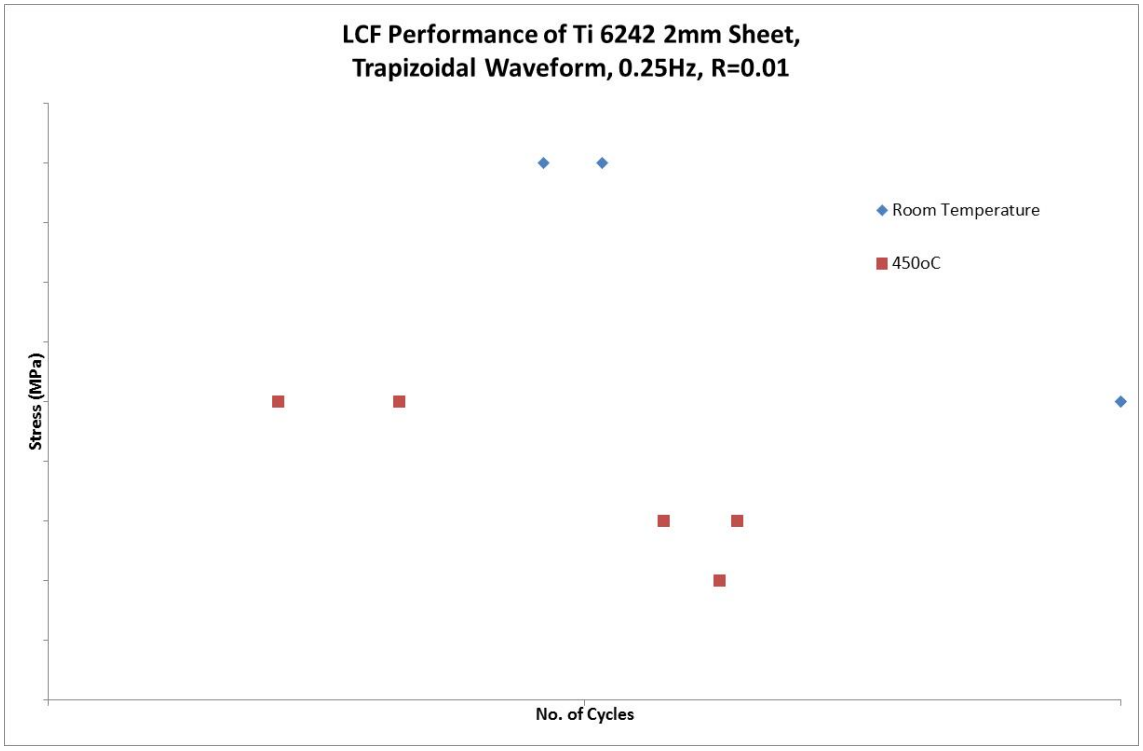

Figure 31 Peak stress versus cycles to failure for Ti-6242S 2mm sheet product

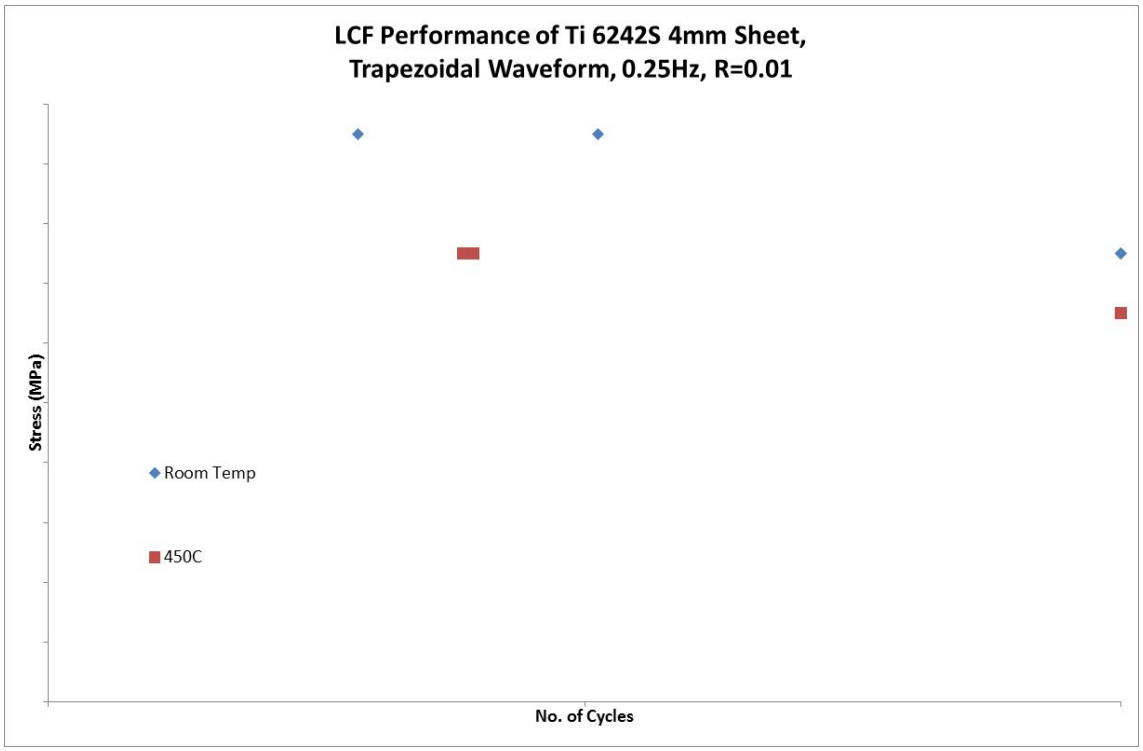

Figure 32 Peak stress versus cycles to failure for Ti-6242S 4mm sheet product

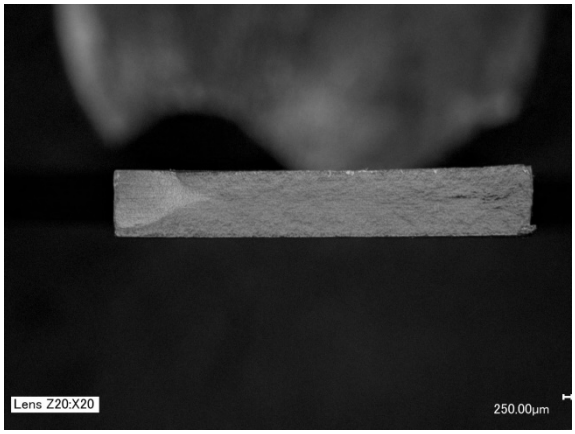

Figure 33 Example of fracture surface of Ti-6242S 2mm sheet elevated temperature premature LCF failures

The room temperature LCF performance of the Ti-834 forged material is illustrated in figure 34. Far shorter fatigue lives were recorded when compared to the sheet and cast variations of the alloy. However it should be noted that the peak strains applied for the forged material were higher than those used for the other Ti-834 variations. A number of different exposure times were used to determine the effect prolonged exposure had on the LCF performance. At the higher strain level there is a notable reduction in the fatigue lives recorded at the longer exposures of 700 and 1000 hours. At the lower strain level there is a lot of scatter in the results where some exposed specimens recorded longer lives than unexposed material. The reduction in fatigue life can be attributed to the oxide and alpha case layers that build up at the surface of the material after prolonged exposure at elevated temperature. This hard brittle layer which has higher oxygen content than the bulk of the alloy is easily cracked and leads to early crack initiation. These results are in line with previous studies [4], which showed that the degradation of fatigue life increased in line with longer exposure and the increasing thickness alpha case layer.

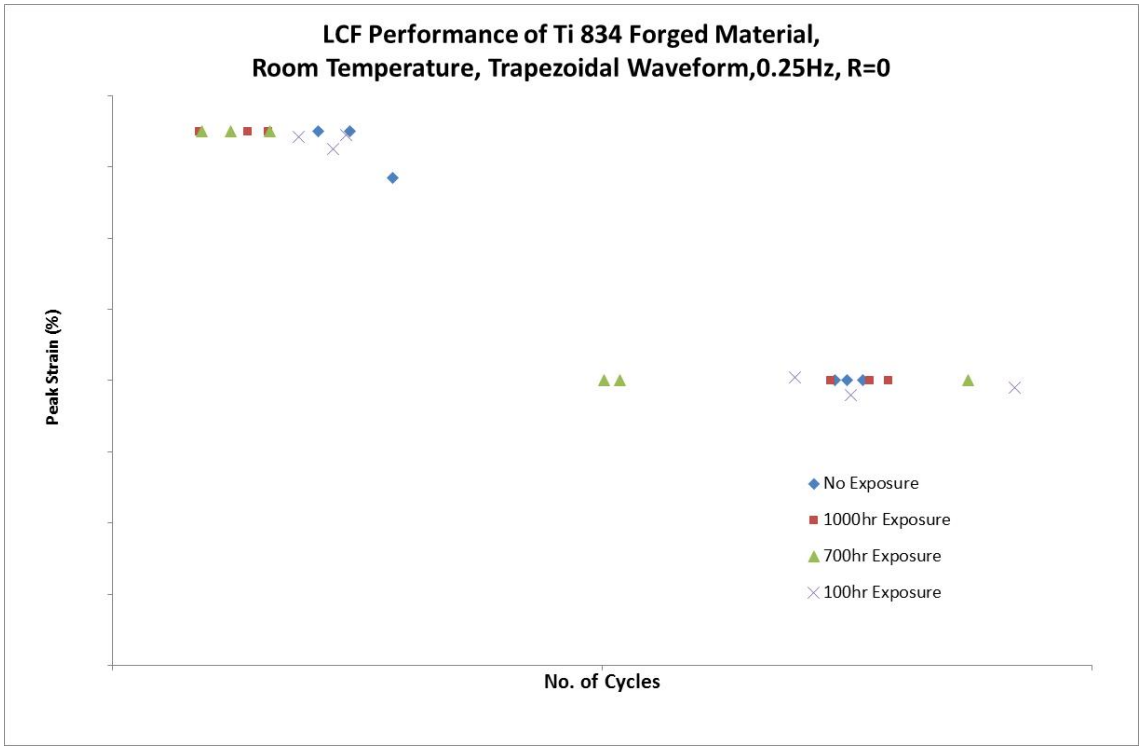

Figure 34 Room temperature peak strain versus cycles to failure for Ti-834 forged material

Higher peak strains were again used for LCF tests on the forged material at elevated temperature (figure 35), as noted at room temperature an exposure of 100 hours had little effect on the LCF performance of the alloy.

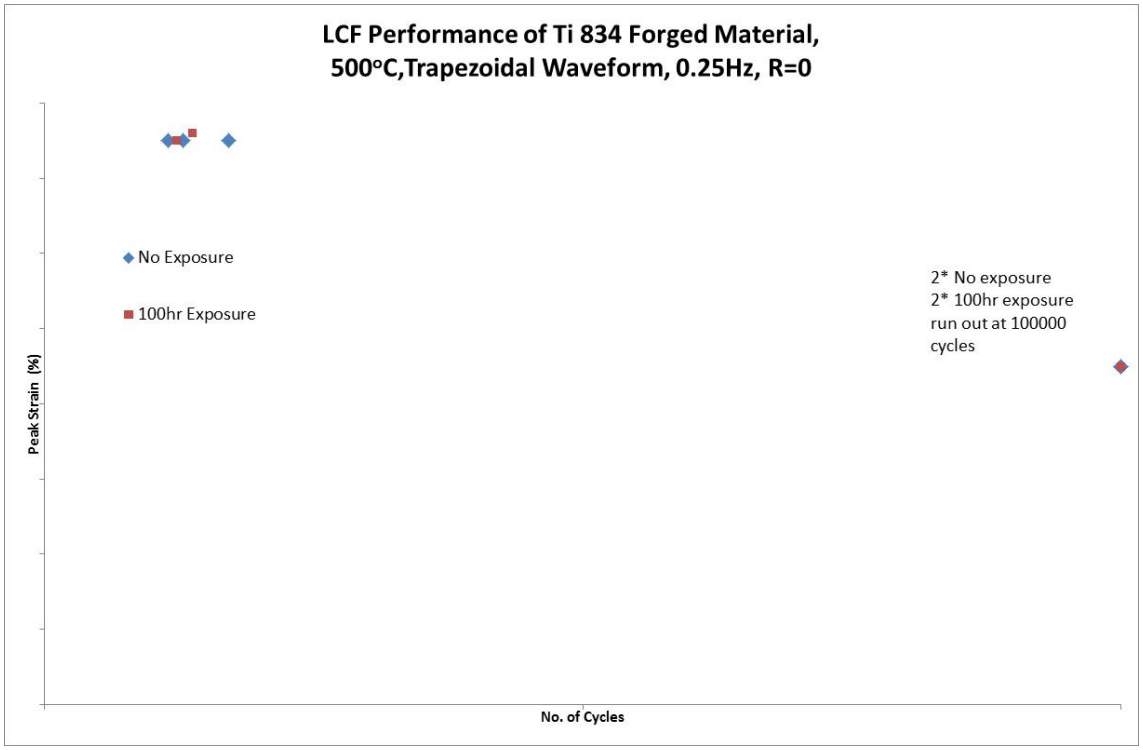

Figure 35 Elevated temperature peak strain versus cycles to failure for Ti-834 forged material

The room temperature LCF results for both the centrifugally cast (figure 36) and gravity cast (figure 37) Ti-834 alloys were disappointing, especially so for the gravity cast material. Short fatigue lives were recorded at both strain levels in both materials in the unexposed condition. Exposure for 500 hours was found to have a significant effect on the fatigue life, especially on the gravity cast material which failed on the first cycle under both strain levels. The reduction in fatigue life for the unexposed material can be attributed to the lamellar microstructure found in the alloys. The bimodal microstructure found in the forged and sheet materials provides very short effective slip lengths within the α phase and crack retardation at α_p/transformed β boundaries. This contrasts to the lamellar microstructures of the cast alloys which provide long effective slip lengths. EBSD analysis of the centrifugally cast alloy shown in figure 38 illustrates that misorientation angles between α lamellae in this alloy are extremely small; where large numbers of α lamellar within each colony were found to have very similar orientations, resulting in very low angle grain boundaries between them. The misorientation angles are shown for L1 (Line 1) and L2 (Line 2) in the same figure. It is clear that the average misorientation angle between the α lamellaes is 0.6^0in L1 and 0.9^0 in L2. This results in far longer effective slip lengths in the cast alloy (~ 450 µm) than those in the forged alloy (~ 20 µm) using statistical average assumption. Therefore it is not surprising that crack propagation in the lamellar microstructure of the cast alloys cast is much faster than in the bimodal microstructures. The lamellar morphology provides an easy crack path through each colony with no

deviation; only arresting when they encounter prior β grain boundaries or other α colonies with vastly different orientations.

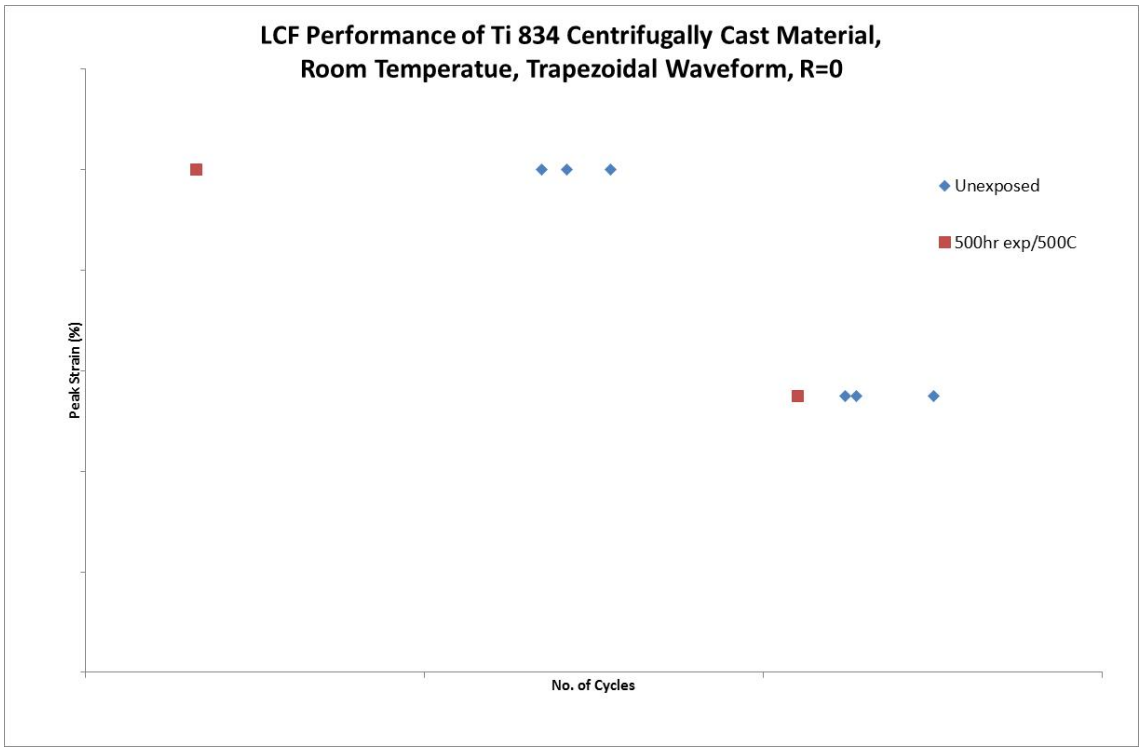

Figure 36 Room temperature peak strain versus cycles to failure for Ti-834 centrifugally cast material

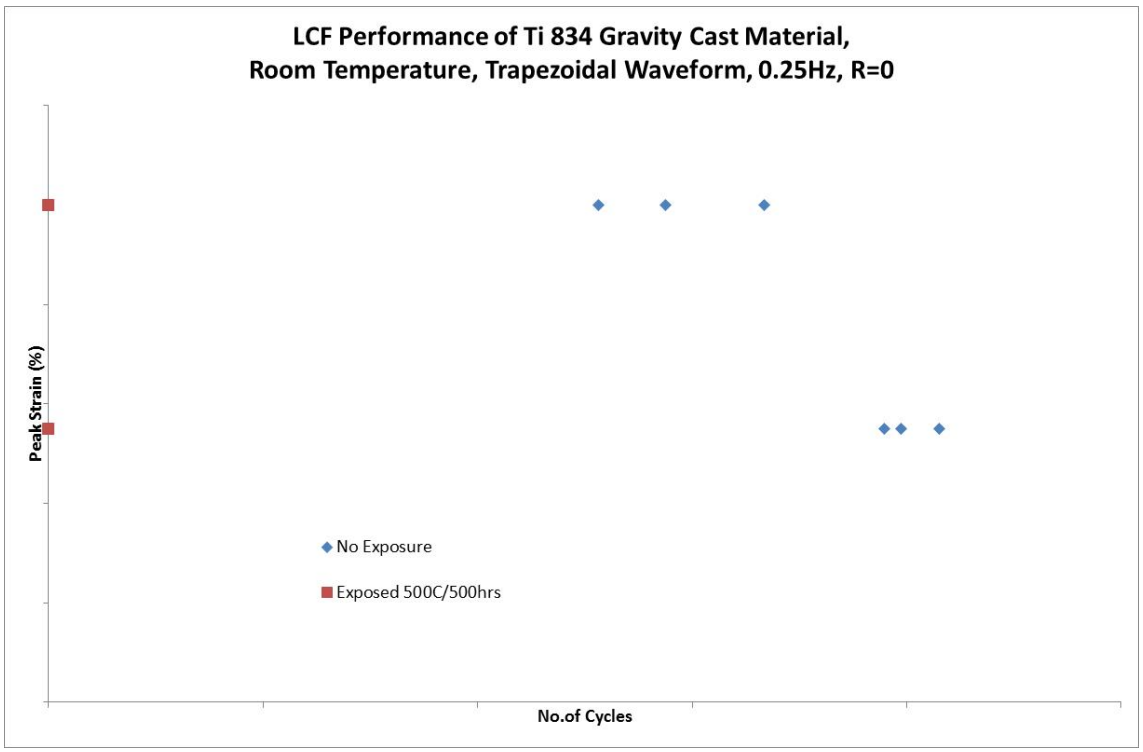

Figure 37 Room temperature peak strain versus cycles to failure for Ti-834 gravity cast material

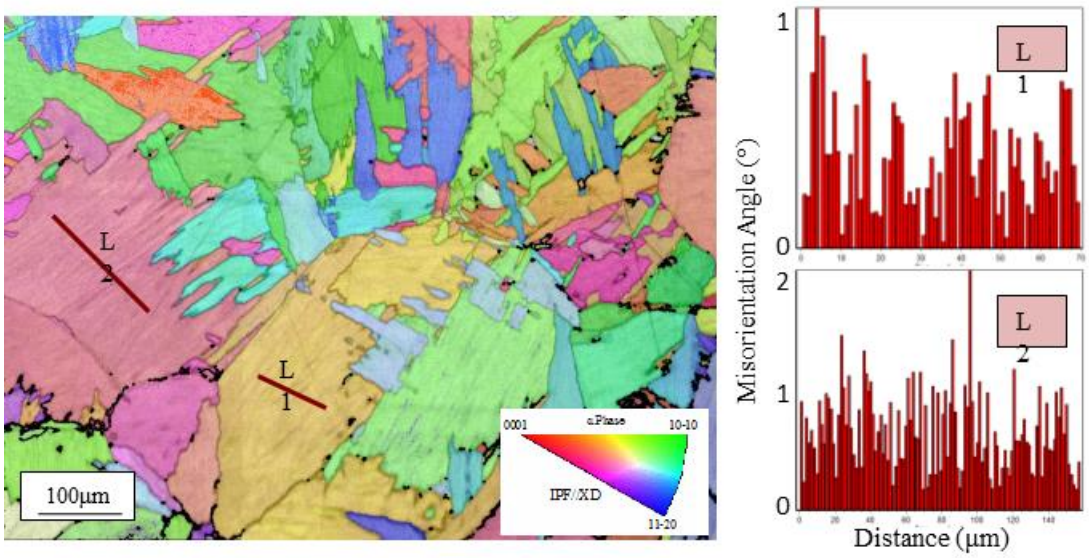

Figure 38 EBSD orientation map of Ti-834 centrifugally cast material

The LCF performance of both the Ti-834 2mm and 4mm welded sheet shown in figure 39 was severely compromised by the condition of the weld in all the plates. As illustrated in figure 40c the microstructure of the HAZ was very coarse when compared to the base sheet material (figure 40b). As a result cracks initiated very early and propagated quickly through this region leading to complete failure through the HAZ area of each specimen every test specimen. An example of this is shown in figure 41.

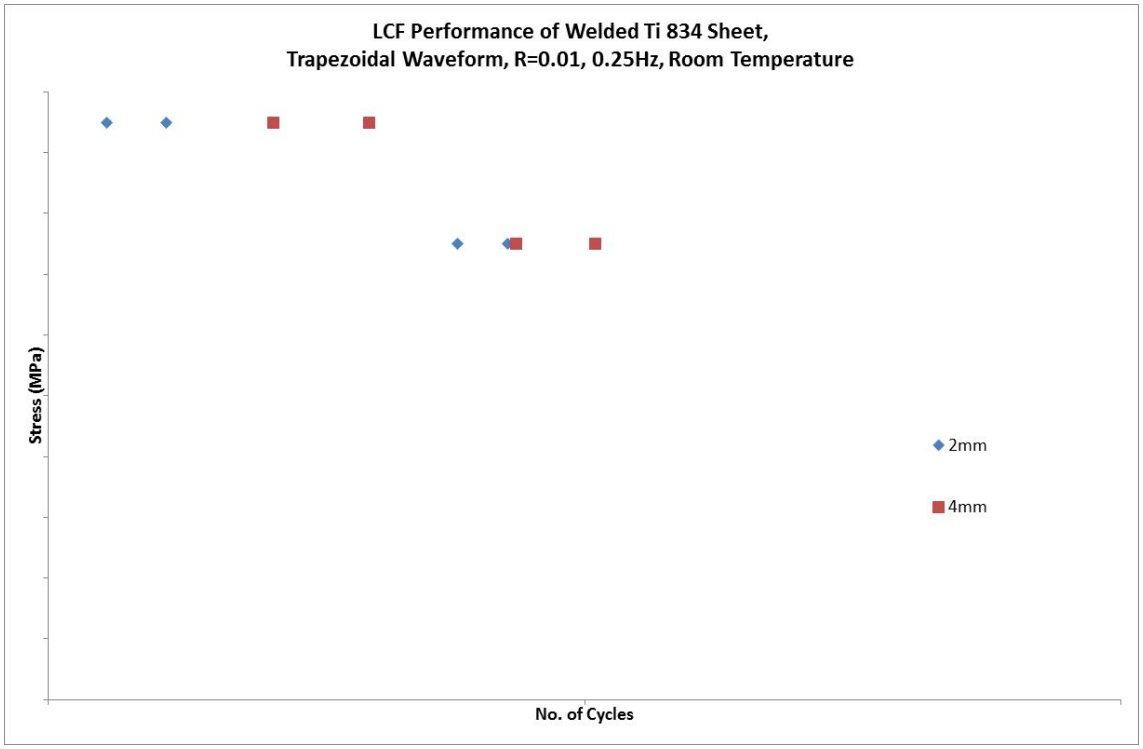

Figure 39 Room temperature peak stress versus cycles to failure for Ti-834 welded sheet material

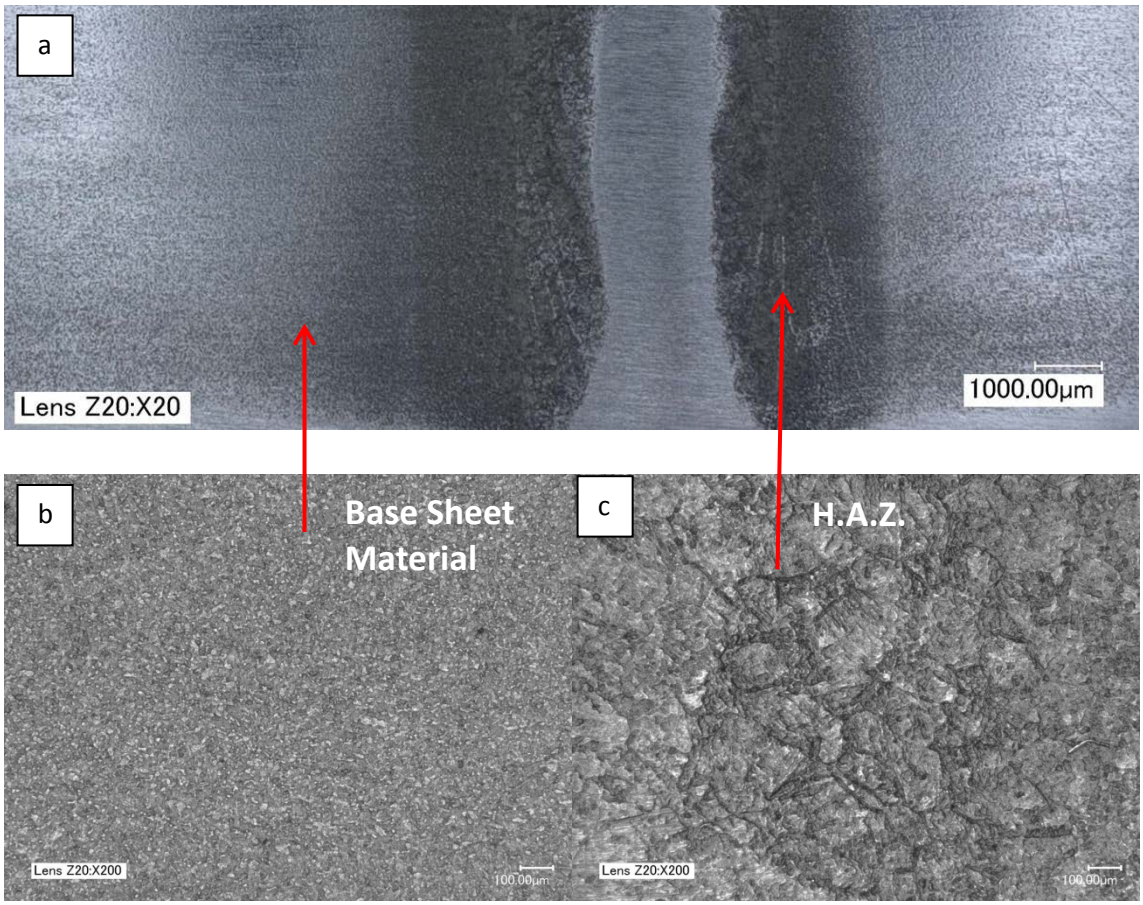

Figure 40 Images of Ti-834 2mm welded sheet

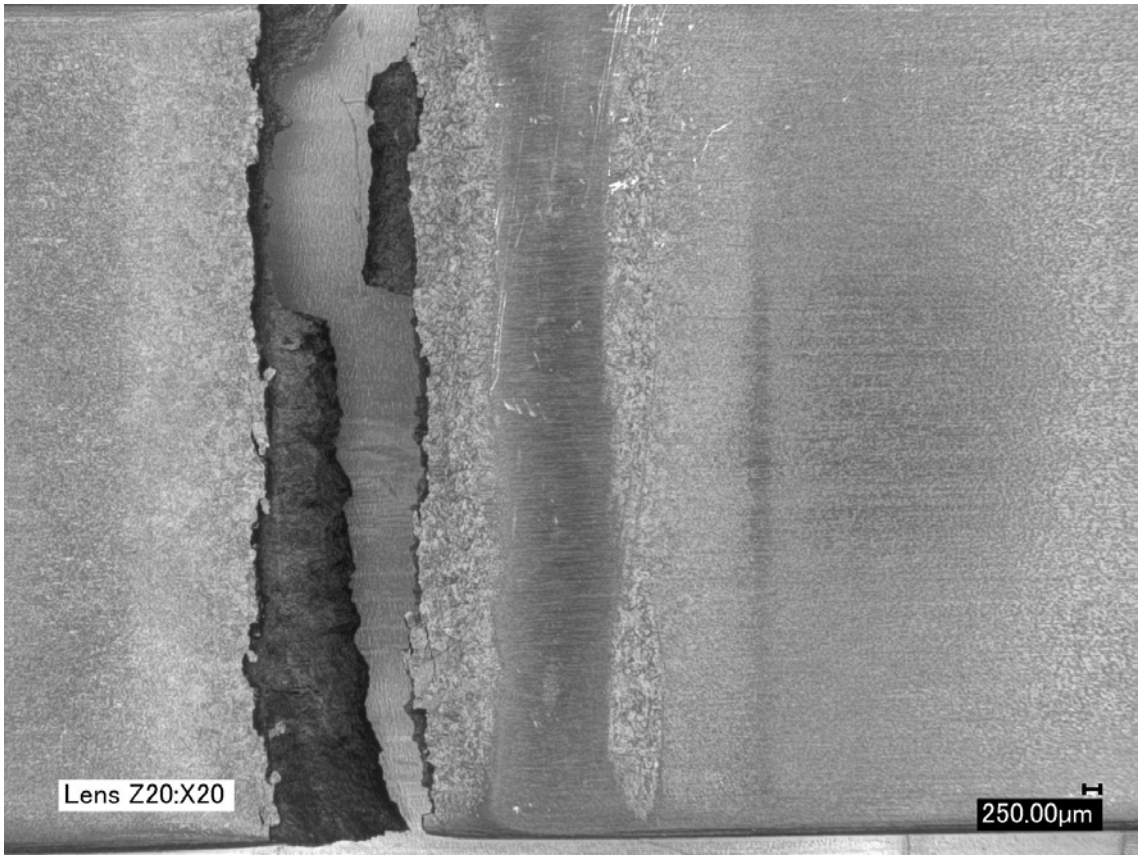

Figure 41 Example of fracture location in Ti-834 welded sheet LCF specimens

The limited creep results attained during the project proved inconclusive, testing being stopped in order to concentrate on the ductility issues with the Ti-834 cast material. The results recorded did not deliver a clear picture of the creep performance of the alloys as there were large discrepancies between the tests. Initial testing on Ti-6242S had determined that the Ti-834 alloys were required to remain on test for at 500^{o}C for 167 hours before accumulating 0.5% creep at 600MPa. However when comparison tests were done on Ti6242S cast material there was a large deviation in the time taken to accumulate 0.5% creep strain. Large strains of over 2% were seen for the Ti6242S cast material on loading at a stress of 600 MPa, this is not surprising as the stress levels employed are above the proof strength of the material at 450^{o}C. Results for the Ti-834 forged material continued to provide variable results. The centrifugally cast Ti-834 alloy was tested at lower stresses than initially intended as the proof stress at 500^{o}C was approximately 100MPa below the intended stress. The creep performance of the alloy was below what was initially required. The gravity cast materials creep performance was far poorer than the centrifugally cast material.

A limited amount of fatigue crack propagation testing was performed during the project; these results are illustrated in figure 42. These results show that the Ti-6242S 25mm centrifugally cast

material has the lowest FCP rate of the 5 materials tested. The Ti-6242S 13mm, Ti-834 centrifugally and gravity cast materials all have similar intermediate FCP rates. Unsurprisingly the Ti-834 forged material with the bimodal microstructure displays the fastest FCP rate of all the materials. The curve for this material is much smoother that those displayed by the cast materials whose curves are characterized by a rougher profile. This can be explained by cracks advancing quickly through the aligned lamellar structures relatively unhindered until they encounter grain boundaries; where their growth is retarded before accelerating once again through the large prior B grains. This is illustrated in figures 43 a & b where the forged material has a smooth crack profile compared to the rough jagged profile of the cast material.

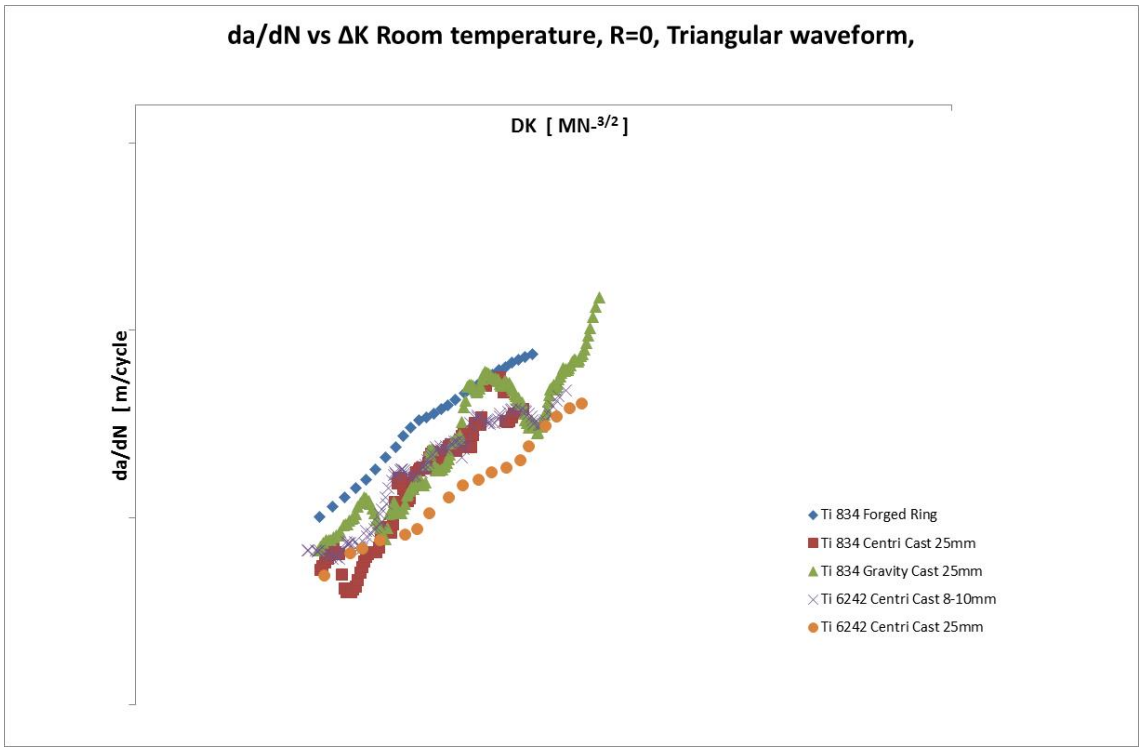

Figure 42 Room temperature FCP result for all materials

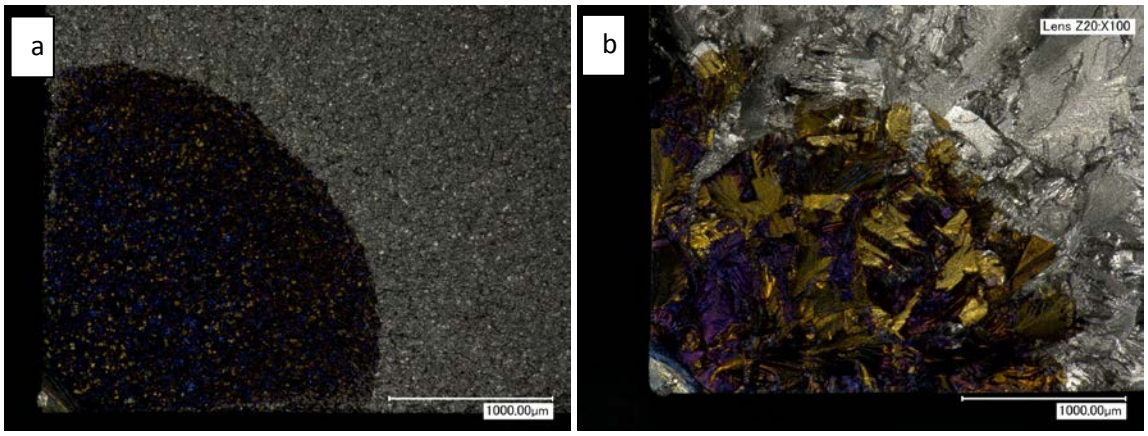

Figure 43 Crack path of a) Ti-834 forged material, b) Ti-834 centrifugally cast material

5. Summary

Initial monotonic testing of the Ti-834 cast material provided positive results, the material demonstrated good ductility and strength at both room and elevated temperatures, and appeared capable of replacing Ti-6242S as an intermediate compressor casing material. Although its LCF performance caused some concern; the effect of long term exposure at the intended operating temperature on ductility is the major obstacle in its way. While the cast form of Ti-6242S maintains approximately 10% ductility at room temperature after 1000 hours exposure at its operating temperature, centrifugally cast Ti-834 only provides approximately 2% ductility after 500 hours exposure at 500^{o}C

The hydrogenation process performed to improve mechanical properties by modifying the grain size of the Ti-834 centrifugally cast material was successful in as far as the structure produced by the process. However the fact that some samples were cracked after the HDH process, and excessive hydrogen was still present after the de gassing stage of the process compromised its mechanical performance. Two tensile tests illustrated that it was possible to modify the structure and attain good mechanical properties in the material via this process. However its practicality as an industrial process must be questioned as it proved unable to reproduce a suitably crack and hydrogen free end product.

The forged variation of the Ti-834 material performed well both in the unexposed and exposed conditions retaining good strength and excellent ductility during tensile tests at both room and elevated temperature. The LCF performance appeared not to be as strong as the Ti-6242S alloy but this was at higher strain levels than those applied to the Ti-6242S material.

Both the 2mm and 4mm sheet variants of the Ti-834 alloy performed well, they both proved to be stronger with similar ductility to the Ti-624S sheet alloys at room temperature while having slightly lower strength at elevated temperature. Prolonged exposure was not found to affect the ductility of either sheet material significantly. The LCF performance was also found to be comparable to the Ti-6242S alloy at both room and elevated temperatures.

The tensile performance of the welded Ti-834 sheets was generally good when fracture occurred away from the HAZ, when fracture occurred in this region ductility was compromised. However due to the poor quality of the microstructure in the HAZ, the LCF performance was significantly below the performance required.

The gravity cast variation of the material was not a viable option as a replacement for Ti-6242S with very poor tensile and LCF performance especially after prolonged exposure at 500^{o}C. This may have

been somewhat expected after studying the microstructure of the material with very large grain size with coarse α laths.

References

[1] C.E. Shamblen, “Embrittlement of Ti Alloys by Long Time, High Temperature Exposure.pdf,” *Metall. Trans.*, vol. 2, pp. 277–280, 1971.

[2] R. Gaddam, B. Sefer, R. Pederson, and M.-L. Antti, “Study of alpha-case depth in Ti-6Al-2Sn-4Zr-2Mo and Ti-6Al-4V,” *IOP Conf. Ser. Mater. Sci. Eng.*, vol. 48, 2013.

[3] Z. Abdallah, K. Perkins, and S. Williams, “Alpha-case kinetics and surface crack growth in the high-temperature alloy Timetal 834 under creep conditions,” *Metall. Mater. Trans. A Phys. Metall. Mater. Sci.*, vol. 43, no. 12, pp. 4647–4654, 2012.

[4] R. Gaddam, M. L. Antti, and R. Pederson, “Influence of alpha-case layer on the low cycle fatigue properties of Ti-6Al-2Sn-4Zr-2Mo alloy,” *Mater. Sci. Eng. A*, vol. 599, pp. 51–56, 2014.

[5] A. L. Pilchak, W. J. Porter, and R. John, “Room temperature fracture processes of a near-?? titanium alloy following elevated temperature exposure,” *J. Mater. Sci.*, vol. 47, no. 20, pp. 7235–7253, 2012.

[6] W. T. Donlan, J. E. Allison, and J. V. Lasecki, “The Influence of Thermal Exposure on Properties and Microstructure of Elevated Temperature Titanium alloys,” in *Titanium 92*, 1992, pp. 295–302.

[7] M. A. Daeubler, D. Helm, and G. Lutjering, “Influence of Heat Treatment on Microstructure and Mechanical Properties of Cast IMI 834,” in *Titanium 95*, 1995, pp. 709–716.

[8] C.Andres, A.Gysler, and G.Lutjering, “Correlation Between Microstructure and Creep Behavior of the High Temperature Ti Alloy IMI 834.”

[9] G. Lütjering, “Influence of processing on microstructure and mechanical properties of (α+β) titanium alloys,” *Mater. Sci. Eng. A*, vol. 243, no. 1–2, pp. 32–45, 1998.

Appendix

a)

BS EN 6892-1:2009	Metallic materials – Tensile testing Part 1: Method of Test at ambient temperature
BS EN ISO 6892-2:2011	Metallic materials. Tensile testing. Method of test at elevated temperature
BS EN 2002-1:2005	Aerospace series. Metallic materials. Test methods. Tensile testing at ambient temperature
BS EN 2002-2:2005	Aerospace series. Metallic materials. Test methods. Tensile testing at elevated temperature

b)

BS 3518-1:1993	Methods of Fatigue Testing
BS 6072:2010	Aerospace series – Metallic materials –Test methods – Constant amplitude fatigue testing
ISO12106:2003	Metallic materials - Fatigue testing. Strain control axial fatigue method.
prEN 3874:1996	Draft European Aerospace Standard - Test methods for metallic materials - Constant amplitude force-controlled low cycle fatigue testing

c)

BS EN ISO 7500-1: 2004	The standard related to the verification of the materials testing machines in tension and compression for increasing forces only. The force verification equipment is calibrated to ISO 376:2002.
BS EN ISO 9513:2012	Methods for the calibration and grading of extensometers for the testing of metals.
BS1041: Part 4	Temperature measurement. Guide to the selection and use of thermocouples.

BS EN 60584-1:1996, IEC 60584-1:1995 Thermocouples. Reference tables.

BS 7270: 2006	Metallic materials. Constant amplitude strain controlled axial fatigue.
ISO12106: 2003	Metallic materials - Fatigue testing. Strain control axial fatigue method.

d)

BS EN ISO 7500-2:2006	Tension creep testing machines – verification of applied load.

BS EN ISO 204:2009 Metallic materials – Uniaxial creep testing in tension

BS EN 2002-005:2007 Aerospace series – Test methods for metallic materials. Part 005: Uninterrupted creep and stress-rupture testing.

BS EN ISO 9513:2012 Metallic materials – Calibration of extensometer systems used in uniaxial testing

e)

BS ISO 12108:2012, Metallic materials – fatigue testing – fatigue crack growth method